



# LUND UNIVERSITY

## Rational Approach to Fire Engineering Design of Steel Buildings

Pettersson, Ove; Magnusson, Sven Erik; Thor, Jörgen

1981

[Link to publication](#)

*Citation for published version (APA):*

Pettersson, O., Magnusson, S. E., & Thor, J. (1981). *Rational Approach to Fire Engineering Design of Steel Buildings*. (LUTVDG/TVBB--3002--SE; Vol. 3002). Division of Building Fire Safety and Technology, Lund Institute of Technology.

*Total number of authors:*

3

### General rights

Unless other specific re-use rights are stated the following general rights apply:

Copyright and moral rights for the publications made accessible in the public portal are retained by the authors and/or other copyright owners and it is a condition of accessing publications that users recognise and abide by the legal requirements associated with these rights.

- Users may download and print one copy of any publication from the public portal for the purpose of private study or research.
- You may not further distribute the material or use it for any profit-making activity or commercial gain
- You may freely distribute the URL identifying the publication in the public portal

Read more about Creative commons licenses: <https://creativecommons.org/licenses/>

### Take down policy

If you believe that this document breaches copyright please contact us providing details, and we will remove access to the work immediately and investigate your claim.

LUND UNIVERSITY

PO Box 117  
221 00 Lund  
+46 46-222 00 00

LUND INSTITUTE OF TECHNOLOGY · LUND · SWEDEN  
DIVISION OF BUILDING FIRE SAFETY AND TECHNOLOGY  
REPORT LUTVDG/(TVBB - 3002)

OVE PETTERSSON - SVEN ERIK MAGNUSSON -  
JÖRGEN THOR

RATIONAL APPROACH  
TO FIRE ENGINEERING DESIGN  
OF STEEL BUILDINGS

LUND 1981

LUND INSTITUTE OF TECHNOLOGY • LUND • SWEDEN

DIVISION OF BUILDING FIRE SAFETY AND TECHNOLOGY

REPORT LUTVDG/(TVBB-3002)

OVE PETTERSSON - SVEN ERIK MAGNUSSON - JÖRGEN THOR

## RATIONAL APPROACH TO FIRE ENGINEERING DESIGN OF STEEL BUILDINGS

Presented at a workshop "Engineering Applications of Fire Technology", April 16-18, 1980, at National Bureau of Standards, Gaithersburg, Maryland, USA

LUND 1981

## Preface

The present paper describes a rational analytical approach to a fire engineering design of load-bearing structures and partitions. The design method is permitted to be generally applied in Sweden, as one alternative, since about ten years. The method is directly based on the natural fire concept and strictly defined functional requirements and performance criteria.

For facilitating the practical application of the design method to steel structures, a comprehensive design basis has been worked out in the form of diagrams and tables for a direct and quick determination of the maximum steel temperature during a complete compartment fire and the corresponding design load-bearing capacity of the fire exposed structure. The design basis is presented in a manual [4] which is approved for practical use by the National Swedish Board of Physical Planning and Building.

The paper is organized in such a way, that a reader, who only wants to be informed of the practical application of the design method, can limit himself to a study of chapter 3 and the explanatory example. Chapters 1 and 2 are supplementing this description with respect to the general design philosophy behind the design method and the connected structural fire safety characteristics.

## Table of Contents

Preface	p 1
Table of Contents	p 2
Introduction	p 4
1. Main Principles of an Analytical Design of Fire Exposed Load-Bearing Structures	p 5
2. Fire Safety of Load-Bearing Structures	p 9
3. Detailed Description of a Differentiated, Analytical Fire Engineering Design of Steel Structures	p 15
3.1 Fire Load Density and Gas Temperature-Time Curves of Fully Developed Compartment Fire	p 17
3.2 Opening Factor $A\sqrt{h}/A_t$	p 21
3.3 Design Temperature State of Fire Exposed, Uninsulated Steel Structures	p 23
3.4 Design Temperature State of Fire Exposed, Insulated Steel Structures	p 26
3.5 Design Temperature State of Fire Exposed Floor or Roof Assembly with Suspended Ceiling	p 28
3.6 Design Temperature State of Fire Exposed Partitions	p 30
3.7 Design Load Effect and Design Load-Bearing Capacity of Fire Exposed Steel Structures	p 33
4. Concluding Remarks	p 38
Example	p 40
References	p 53
Appendix	
<u>Table A1.</u> Fire load characteristics according to recent Swedish investigations. Design fire load density	p A1



<u>Table A2.</u> Coefficient $K_f$ for transforming a real fire load density and a real opening factor of a fire compartment to effective values, corresponding to a fire compartment, type A	p A2
<u>Table A3.</u> Maximum steel temperature for uninsulated steel structure as function of compartment fire and structural characteristics	p A4
<u>Table A4.</u> $F_s/V_s$ for different types of fire exposed, uninsulated steel structures	p A5
<u>Table A5.</u> Maximum steel temperature for insulated steel structure as function of compartment fire and structural characteristics	p A6
<u>Table A6.</u> Thermal conductivity of some insulation materials as function of insulation temperature	p A8
<u>Table A7.</u> Maximum steel temperature for steel structure, insulated with mineral wool slabs ( $\rho_i=150 \text{ kg m}^{-3}$ ), as function of compartment fire and structural characteristics	p A9
<u>Table A8.</u> $A_i/V_s$ for different types of fire exposed, insulated steel structures	p A10
<u>Table A9.</u> Maximum steel beam temperature for a floor or roof assembly with suspended ceiling, as function of compartment fire and structural characteristics	p A11
<u>Table A10.</u> Effective $d_i/\lambda_i$ and critical temperature for some types of suspended ceilings	p A12
<u>Table A11.</u> Load values to be applied in a differentiated, analytical, structural fire engineering design	p A13

## RATIONAL APPROACH TO FIRE ENGINEERING DESIGN OF STEEL BUILDINGS

By Ove Pettersson and Sven Erik Magnusson, Department of Structural Mechanics, Lund Institute of Technology, Lund, Sweden, and Jörgen Thor, Swedish Institute of Steel Construction, Stockholm, Sweden

A development of analytical design procedures, based on well-defined functional requirements, is an important task of the future fire research within different fields of the overall fire safety concept. Such procedures, successively replacing the present, internationally prevalent, schematic design methods, are necessary for getting an improved economy and for enabling more qualified and reliable fire safety analyses. A derivation of such analytical design systems is also in agreement with the present trend of development of the building codes and regulations in many countries towards an increased extent of functionally based requirements and performance criteria.

In the ideal case, a rational fire design methodology includes as essential components [1]

- \* analytical modelling of relevant processes; verification of model validation and accuracy; determination of critical design parameters,
- \* formulation of functional requirements, independent of choice of design process and expressed either in deterministic or probabilistic terms,
- \* determination of design parameter values, and
- \* verification by the means of a reliability analysis that the choice of safety factors leads to safety levels, which are consistent with the expressed functional requirements.

For a fire engineering design of load-bearing structures and partitions, a differentiated analytical procedure is permitted to be applied in Sweden, as one alternative, since about ten years. The procedure constitutes a direct design method based on temperature characteristics of the fully developed compartment fire as a function of the fire load density, the

ventilation of the fire compartment and the thermal properties of the structures enclosing the fire compartment. The design method is approved for a general practical use by the National Swedish Board of Physical Planning and Building [2]. For facilitating the practical application, design diagrams and tables are systematically produced, giving directly, on one hand, the design temperature state of the fire exposed structure, on the other, a transfer of this information to the corresponding design load-bearing capacity of the structure; c.f., for instance [3], [4], [5], [6]. Fig. 1 describes the design method in a summary way.

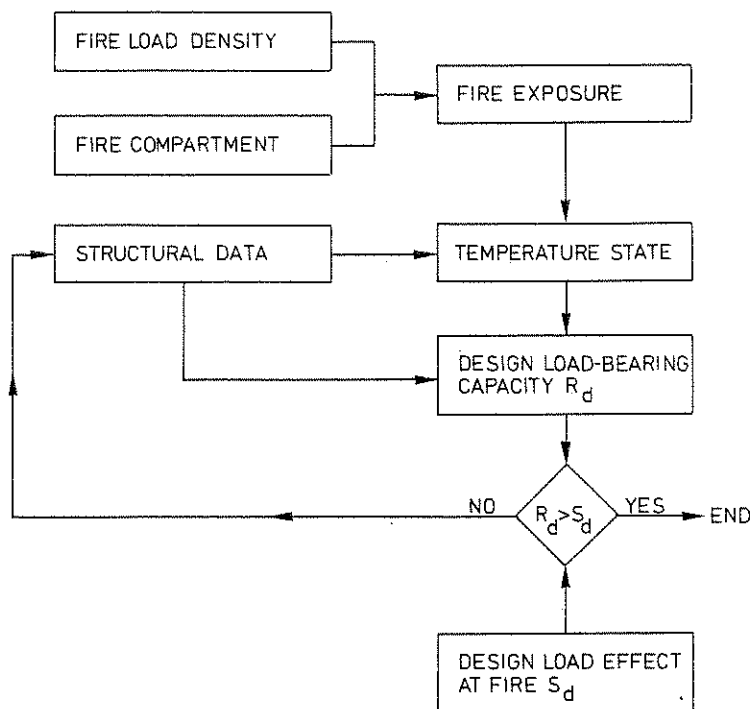


Figure 1. Summary description of a rational design method for fire exposed load-bearing structures

### 1. Main Principles of an Analytical Design of Fire Exposed Load-Bearing Structures

In a generalized summary way, an analytical design method for fire exposed structures, based on well-defined functional requirements, can be described according to Fig. 2.



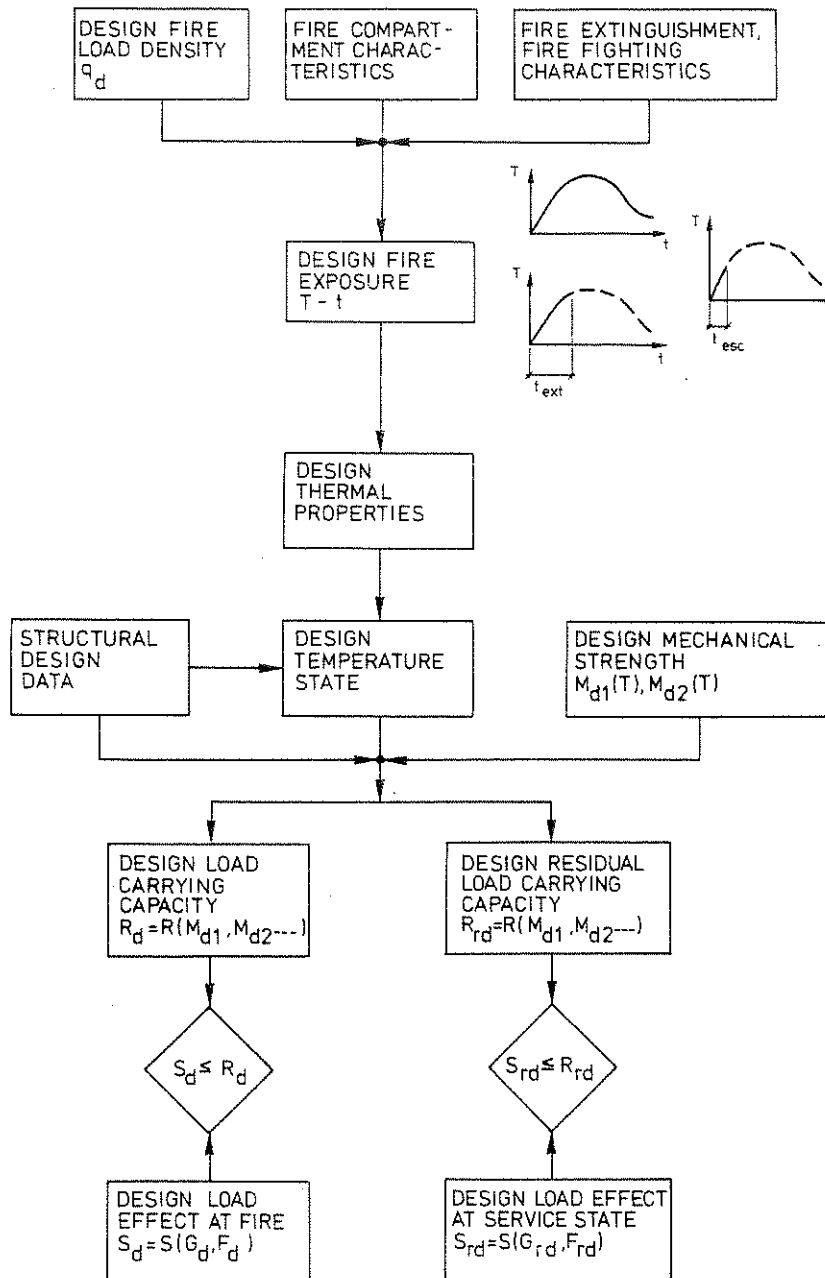


Figure 2. Procedure of a rational, reliability-based design of fire exposed load-bearing structures [1]

The design fire load density, the fire compartment characteristics and the fire extinguishment and fire fighting characteristics constitute the basis for a determination of the design fire exposure, given as the gastemperature-time curve  $T-t$  of the fully developed compartment fire. Depending on the type of practical application, the load-bearing function of the structure can be required to be fulfilled for

- \* the complete fire process,
- \* a shortened fire process, limited by the time  $t_{\text{ext}}$ , necessary for the fire to be extinguished under the most severe conditions, or
- \* a shortened fire process, limited by the design evacuation time  $t_{\text{esc}}$  for the building.

Together with the structural design data, the design thermal properties and the design mechanical strength of the structural materials, the design fire exposure gives the design temperature state and the design load-carrying capacity  $R_d$  as the lowest value during the relevant fire process.

A direct comparison between the design load-carrying capacity  $R_d$  and the design load effect at fire  $S_d$  decides whether the structure can fulfil its required function or not at the fire exposure. The quantities  $R_d$  and  $S_d$  then both can be referred to a defined load or a decisive section effect, for instance, a bending moment or a shear force.

Following, for instance the new Draft Code for Loading Regulations, issued by the Nordic Committee for Building Regulations [7], the determination of the design load effect  $S_d$  starts from characteristic values of permanent and variable loads  $G_k$  and  $F_k$ , connected to a defined probability of excess during a specified time period (Fig. 3). A multiplication by partial factors  $\gamma$  and load combination factors  $\psi$  transfers the characteristic load values to design loads  $G_d$  and  $F_d$ . The load combination factors  $\psi$  then may be differentiated with respect to whether a complete evacuation of people can be assumed or not in the event of fire. Finally, the design loads are combined and transformed to the design load effect at fire  $S_d$ .

Analogously, the design material strength  $M_d$  is to be calculated via characteristic strength values  $M_k$  at actual temperature, divided by resulting partial factors  $\gamma_m$  (Fig. 4). The characteristic strength values are defined as corresponding to specified fractiles of the probability density distribution. The different partial factors  $\gamma_m^1$ ,  $\gamma_m^2$ ,  $\gamma_m^3$ , and  $\gamma_m^4$ , are expressing the influence of the scatter in material strength, the uncertainty of the design model, the uncertainty in relation between material property in the structure and material property determined in test, and the safety class, respectively. The predicted extent of personal and property damage at failure - very serious, serious, not serious - decides the safety class.

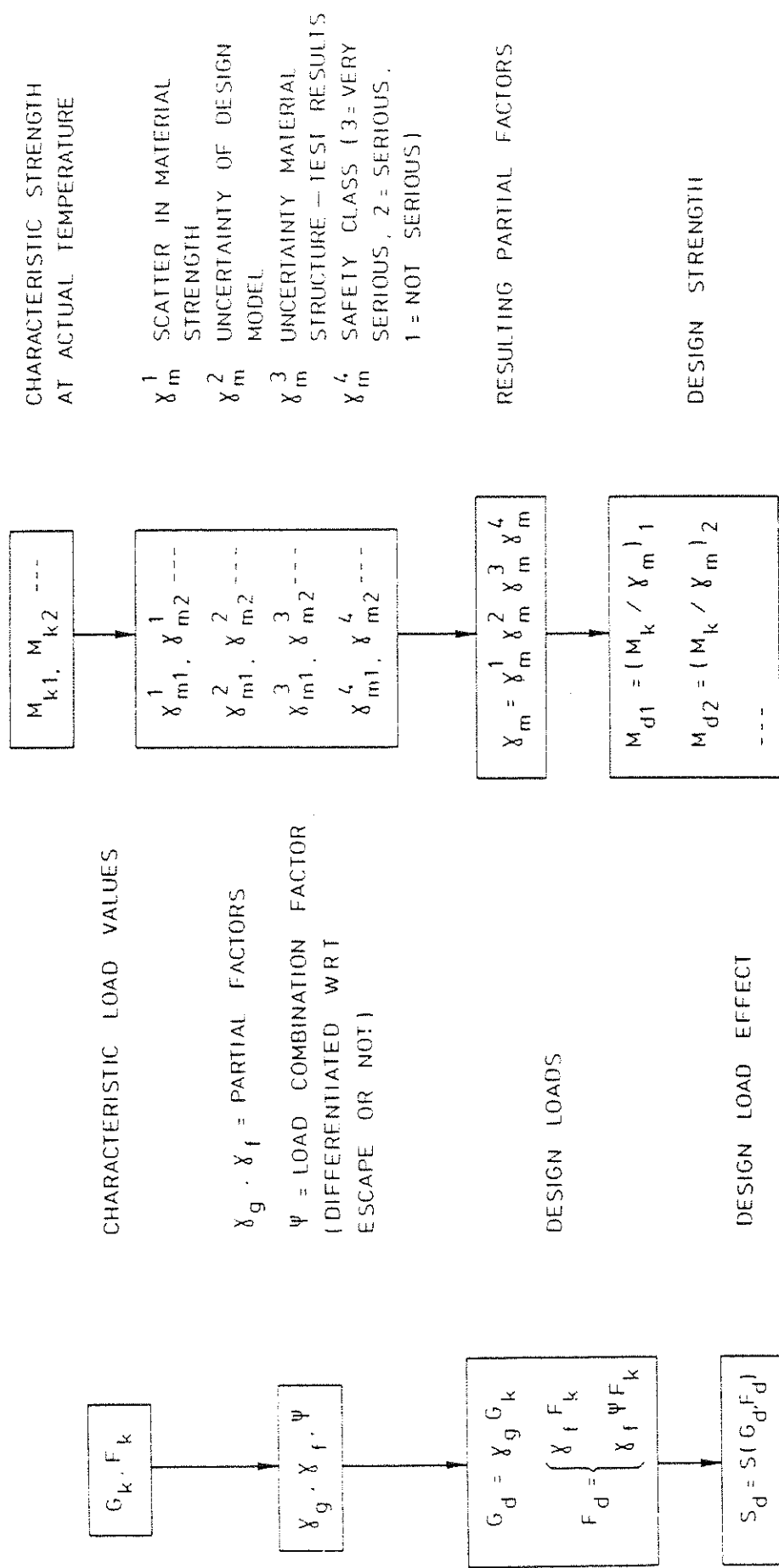


Figure 3. Procedure of determination of design load effect  $S_d$

Figure 4. Procedure of determination of design strength  $M_d$

A similar approach - as outlined for the design load effect  $S_d$  and the design mechanical strength  $M_d$  - can be applied also to the design fire load density  $q_d$  and the design thermal properties of the structural materials.

The level of the functional requirements to be laid down for a structural fire engineering design must be differentiated with respect to such influences as the occupancy, the height and volume of the building, and the importance of the structure or the structural member for the overall stability of the building. This can be met by, for instance, a division of buildings in categories with a related differentiation of the design fire load density and the length of the fire process, to be considered in the design.

For buildings containing activities, which are particularly important from, for instance, an economical point of view, there can be the motive for requiring that the building can be used again after a fire, almost immediately or very soon, for the current activities in a full extent. If the design also comprises such a requirement on re-serviceability of the structure after fire, the design procedure is to be expanded in the following way.

From the time curve of the load-carrying capacity  $R$ , the design residual load-carrying capacity  $R_{rd}$  of the structure after fire is obtained as end information. This quantity  $R_{rd}$  has to be compared with the design load effect at service, non-fire state, on the structure  $S_{rd}$ , given by the corresponding characteristic load values, partial factors and load combination factors.

## 2. Fire Safety of Load-Bearing Structures

In a general sense, the fire engineering design problem is non-deterministic. Performance has to be described and measured in probabilistic terms.

This is one essential perspective from which we have to judge or appraise the building fire safety code systems now in force. Historically, they had to be written without actually stating their objective level of safety and, still far less, without any analytical measurement of the

objectives involved. For this reason, there is an urgent need for future attempts to evaluate the levels of safety inherent in present local and national fire protection regulations and to develop rational, reliability-based design methods, leading to safety levels which are consistent with the relevant functional requirements [1].

For the case that the load-bearing capacity  $R$  and the load effect  $S$  can be expressed analytically, are statistically uncorrelated and have known probability density functions  $f_R$  and  $f_S$ , the probability of failure is given by the formula - cf. Fig. 5

$$P_f = \int_0^\infty \int_0^S f_S(s) f_R(r) ds dr \quad (1)$$

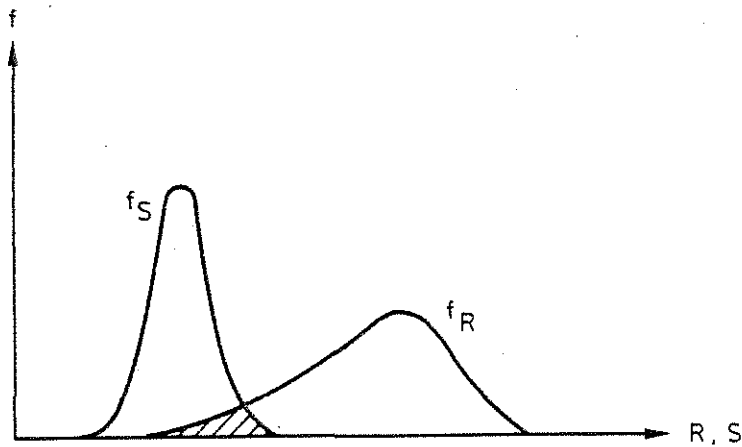


Figure 5. Probability density function  $f_R$  and  $f_S$  of load-bearing capacity  $R$  and load effect  $S$

The computation of the probability of failure  $P_f$  can be re-formulated in the following way - Fig. 6. The difference between the load-bearing capacity  $R$  and the load effect  $S$  defines the safety margin. In the probability density function of the safety margin  $f_{R-S}$ , positive values mean survival, negative values failure. The dashed area gives the failure probability  $P_f$ .

Ideally,  $P_f$  should form the basis for deriving design criteria. However,  $P_f$  can be evaluated accurately only if the probability density function

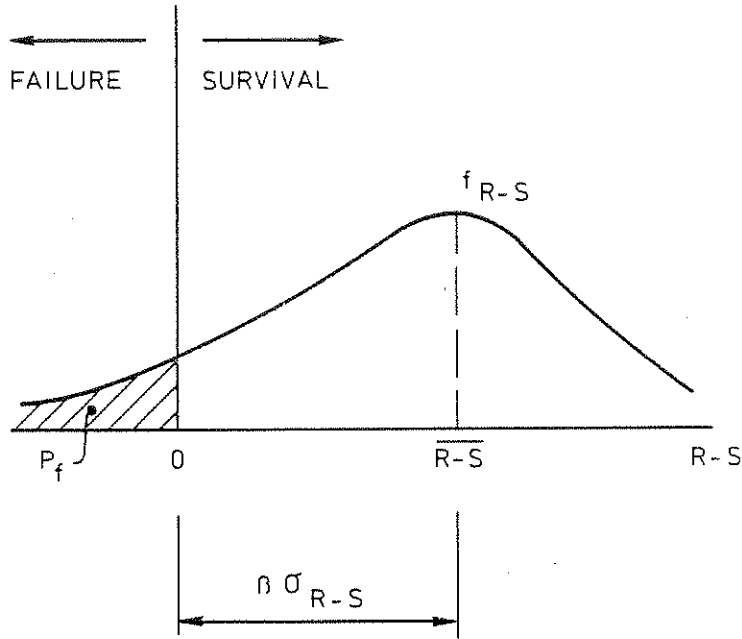


Figure 6. Probability density function  $f_{R-S}$  of safety margin  $R-S$  and definition of safety index  $\beta$

of  $R-S$  is known in detail. In practice, this is very seldom the case. Two main alternatives then are open [8], [9]

- \* to base a design code format on prescribed distributions of  $R$  and  $S$ , and
- \* to acknowledge the incompleteness of statistical information and disregard the form of the distribution involved.

In the latter case, a design scheme can be based simply on requiring that some minimum safety margin be maintained. In place of requiring that a calculated risk of failure must fall below a specified probability, it may be required that the average safety margin  $R-S$  must lie a specified number  $\beta$  standard deviation above zero, giving the formulas

$$\overline{R-S} \geq \beta \sigma_{R-S} \quad \text{or} \quad \bar{R} \geq \bar{S} + \beta \sqrt{\sigma_R^2 + \sigma_S^2} \quad (2)$$

$\sigma_{R-S}$  is the standard deviation of the safety margin  $R-S$ ,  $\sigma_R$  and  $\sigma_S$  are the standard deviation of  $R$  and  $S$ , respectively.

The safety index  $\beta$  defines the reliability of, for instance, a design system. A greater value of  $\beta$  then corresponds to a higher safety level.

With this safety measure we can improve our design methods to be more consistent and assess the implications of assumptions and guesses.

A methodology for a probabilistic analysis of fire exposed steel structures, connected to the design method described in chapter 1, has been developed in [10]. The methodology comprises a general systematized scheme for the identification and evaluation of the various sources and kinds of uncertainty in the differentiated structural fire engineering design. The structure of the methodology is quite general and applicable to a wide class of structures and structural elements. To get applicable and efficient final safety measures, the probabilistic analysis is numerically exemplified for an insulated, simply supported steel beam of I-cross section as a part of a floor or roof assembly. The chosen statistics of dead and live load and fire load density are representative for office buildings.

With the basic data variables selected, the different uncertainty sources in the design procedure are identified and dissembled in such a way that available information from laboratory tests can be utilized in a manner as profitable as possible. The derivation of the total or system variance  $\text{Var}(R)$  in the load-carrying capacity  $R$  is divided into two main stages: variability  $\text{Var}(T_{\max})$  in maximal steel temperature  $T_{\max}$  for a given type of structure and a given design fire compartment, and variability in strength theory and material properties for known value of  $T_{\max}$ .

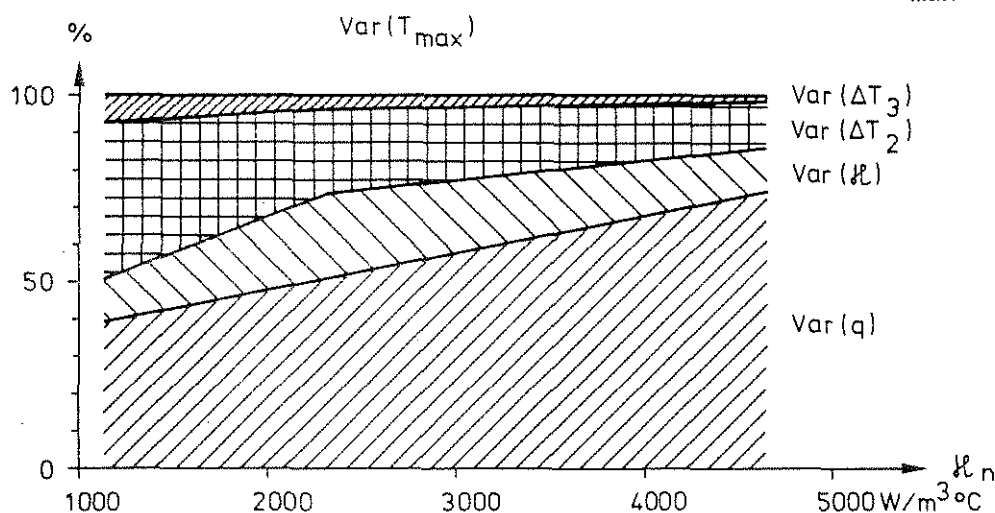


Figure 7. Decomposition of total variance in  $T_{\max}$  into component variances as a function of insulation parameter  $k_n$  [10]



The results obtained are exemplified in Fig. 7, giving the decomposition of the total variance in maximum steel temperature  $T_{\max}$  into the component variances as a function of the insulation parameter  $\kappa_n = A_i \lambda_i / (V_s d_i)$ .  $A_i$  is the interior jacket surface area of the insulation per unit length,  $d_i$  the thickness of the insulation,  $\lambda_i$  the thermal conductivity of the insulating material, corresponding to an average value for the whole process of fire exposure, and  $V_s$  the volume of the steel structure per unit length. Increasing  $\kappa_n$  expresses a decreased insulation capacity.

The component variances refer to the stochastic character of the fire load density  $q$ , the uncertainty in the insulation properties  $\kappa$ , the uncertainty reflecting the prediction error in the theory of compartment fires and heat transfer from the fire process to the structural member  $\Delta T_2$ , and a correction term reflecting the difference between a natural fire in a laboratory and under real life service conditions  $\Delta T_3$ . Analogously, Fig. 8 exemplifies the decomposition of the total variance in the load-carrying capacity  $R$  into component variances as a function of the insulation parameter  $\kappa_n$ . The component variances refer to the variability in the maximum steel temperature  $T_{\max}$ , variability in material strength  $M$ , the uncertainty reflecting the prediction error in the strength theory  $\Delta \phi_1$ , and the uncertainty due to the difference between laboratory tests and in situ fire exposure  $\Delta \phi_2$ .

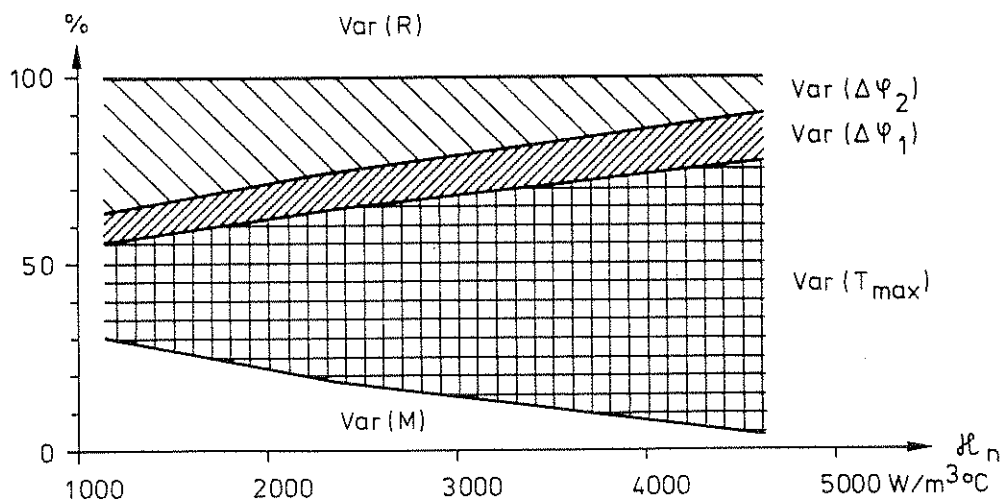


Figure 8. Decomposition of total variance in load-carrying capacity  $R$  into component variances as a function of insulation parameter  $\kappa_n$  [10]

The component variances are quantified, whenever possible by comparing the design theory with experiments. System variance is evaluated in two ways: by Monte Carlo simulation and by use of a truncated Taylor series expansion. Employing the Monte Carlo procedure, the mean and variance of  $R$  and  $S$  have been computed for different values of the ventilation factor of the fire compartment, the insulation parameter  $\kappa$  and the ratio  $D_n/L_n$ , where  $D_n$  is nominal dead load and  $L_n$  nominal live load, used in the normal temperature design. The second moment reliability as a function of these design parameters is evaluated by the safety index formulation according to Eq. (2).

A fragmentary illustration of the results received is given in Table 1, showing the range of variation for the safety index  $\beta$ , as determined for the present Swedish differentiated analytical design model (case II). Varying the opening factor of the fire compartment  $A\sqrt{h}/A_t$  from 0.04 to  $0.12 \text{ m}^{1/2}$  and the ratio between the nominal value of dead load  $D_n$  and live load  $L_n$  from  $1/3$  to  $3$ , then leads to a range of  $\beta$  from  $1.66$  to  $2.84$ .  $A$  is the total area of the window openings,  $h$  the mean value of the heights of window and door openings, weighed with respect to each individual opening area, and  $A_t$  the total interior area of the surface bounding the compartment, opening areas included. For the structural member designed in accordance to the standard fire endurance test (case I), the corresponding range of  $\beta$  will be from  $1.77$  to  $3.69$ . Completing the present differentiated design model with statistically derived load factors (case III) will improve the consistency of  $\beta$  considerably by giving a very narrow range from  $2.35$  to  $2.45$ .

Table 1. Safety index  $\beta$  and probability of failure  $P_f$  for different design procedures, applied to an insulated, simply supported steel beam as a part of a floor or roof assembly in office buildings

Design procedure	Range of $\beta$	Range of $P_f$	$(P_f)_{\max}/(P_f)_{\min}$
I. Classification, standard endurance test	$1.77 - 3.69$	$(1-400)10^{-4}$	$\sim 400$
II. Present Swedish design model	$1.66 - 2.84$	$(23-500)10^{-4}$	$\sim 20$
III = II, improved by statistically derived load factors	$2.35 - 2.45$	$(72-95)10^{-4}$	$\sim 1.5$

The corresponding range of the probability of failure  $P_f$  is shown in the table, too. Related to this quantity, the difference between the three design procedures is extremely striking with the respective ratios  $(P_f)_{\max}/(P_f)_{\min} = 400, 20$  and  $1.5$ . The  $P_f$  values presented are connected to a probability = 1 for a fire outbreak leading to flashover within the fire compartment.

### 3. Detailed Description of a Differentiated, Analytical Fire Engineering Design of Steel Structures

As mentioned in the introduction, a differentiated analytical procedure is permitted to be applied in Sweden for a fire engineering design of load-bearing structures and partitions since about ten years. The main principles behind the design procedure and the connected fire safety aspects are dealt with in the proceeding chapters.

Applied to fire exposed load-bearing structures or structural members, inside a fire compartment, the design procedure includes the following steps - Fig. 9.

The basis of the design is given by the fully developed compartment fire exposure. Decisive entrance quantities then are

- (1) nominal load and load factor for fire load density,
- (2) combustion properties of this design fire load,
- (3) size and geometry of the fire compartment,
- (4) ventilation characteristics of the fire compartment, and
- (5) thermal properties of structures enclosing the fire compartment.

These quantities jointly determine the rate of burning, the rate of heat release, and the design gas temperature-time curve of the complete fire process. Together with

- (6) structural data for the proposed structure,
- (7) thermal properties of structural materials, and
- (8) coefficients of heat transfer for various surfaces of the structure

this design gas temperature-time curve gives the requisite information for a determination of the transient temperature fields of the fire exposed structure or structural members. With

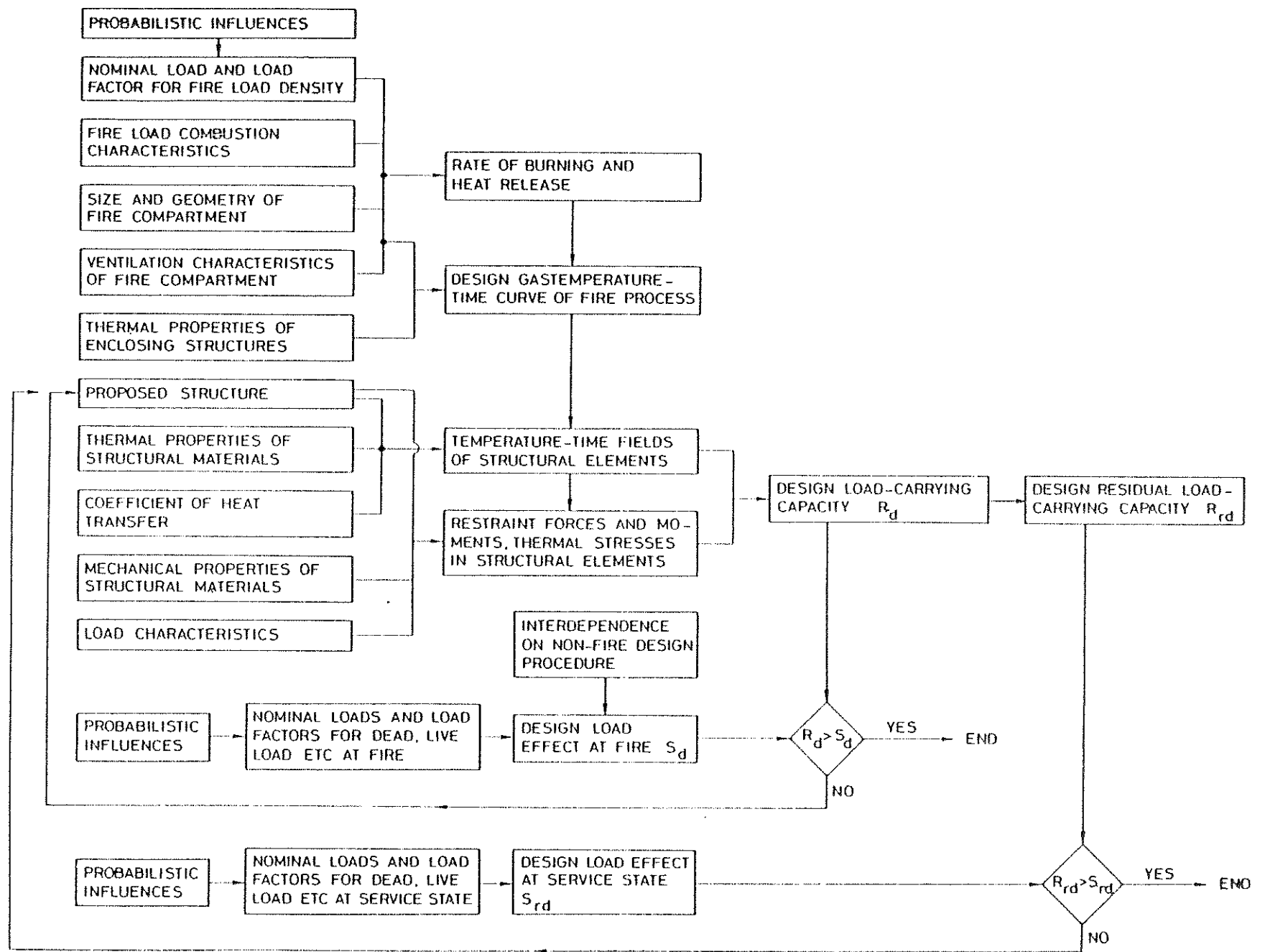


Figure 9. Procedure of a differentiated, analytical fire engineering design of load-bearing structures with additional requirement on re-serviceability after fire

- (9) mechanical properties of structural materials (Fig. 4), and
- (10) load characteristics

as further entrance quantities the time variation of restraint forces and moments, thermal stresses, and load-carrying capacity  $R$  can be determined. The lowest value of  $R$  during the complete fire process defines the design load-carrying capacity  $R_d$ .

Over nominal loads and load factors for dead load, live load, etc, statistically representative of a fire occasion, the design load effect at fire  $S_d$  is defined, interdependent on non-fire design procedure (Fig. 3).

A direct comparison between the design load-carrying capacity  $R_d$  and the design load effect at fire  $S_d$  decides whether the structure can fulfil its required function or not at a fire exposure.

Exceptionally, a requirement on re-serviceability of the structure after fire may be included on the fire engineering design. If so, the design residual load-carrying capacity  $R_{rd}$  of the structure after fire has to be determined in the design and compared with the design load effect at service, non-fire state, on the structure  $S_{rd}$ .

For exterior, load-bearing structures, the procedure for a direct, differentiated design will be modified with respect to the thermal exposure. For such a structure, the transient temperature fields are determined by a combined radiation and convection exposure from the flames and combustion gases outside the fire compartment as well as by radiation from the interior of the fire compartment through its window openings; cf., for instance [11], [12]. For the rest, the design procedure is principally the same as for interior, load-bearing structures.

### 3.1 Fire Load Density and Gas Temperature-Time Curves of a Fully Developed Compartment Fire

At known combustion characteristics of the fire load, the gas temperature-time curve of a fully developed compartment fire can be calculated in the individual practical application from the heat and mass balance equations of the fire compartment with regard taken to the size, geometry and ventilation of the compartment, and to the thermal properties of the structures enclosing the compartment - Fig. 10 [2], [4], [6], [13], [14], [15], [16], [17], [18], [19].

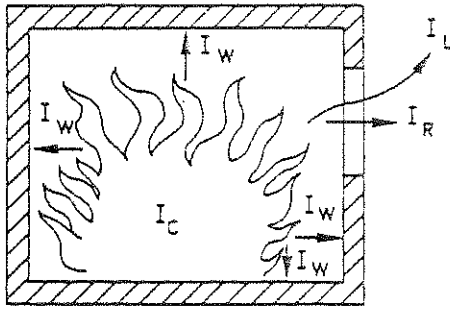


Figure 10. Energy balance equation  $I_C = I_L + I_W + I_R$  of a fire compartment.  $I_C$  is the heat release per unit time from the combustion of the fuel, and  $I_L$ ,  $I_W$  and  $I_R$  the quantities of energy removed per unit time by change of hot gases against cold air, by heat transfer to the surrounding structures, and by radiation through the openings of the compartment, respectively

For interior, load-bearing structures and partitions, the fire engineering design provisionally can be based on gas temperature-time curves  $T_t-t$  according to Fig. 11, [2], [4], [6], [15], which applies to a fire compartment with surrounding structures made of a material with a thermal conductivity  $\lambda = 0.81 \text{ W} \cdot \text{m}^{-1} \cdot ^\circ\text{C}^{-1}$  and a heat capacity  $\rho c_p = 1.67 \text{ MJ} \cdot \text{m}^{-3} \cdot ^\circ\text{C}^{-1}$  (fire compartment, type A). Entrance parameters of the diagrams are the fire load density  $q$ , defined by the formula

$$q = \frac{1}{A_t} \sum \mu_v m_v H_v \quad (\text{MJ} \cdot \text{m}^{-2}) \quad (3)$$

and the ventilation characteristics of the fire compartment, expressed by the opening factor  $A\sqrt{h}/A_t \text{ (m}^{1/2}\text{)}$ , where

- $A$  = total area of window and door openings ( $\text{m}^2$ ),
- $h$  = mean value of the heights of window and door openings, weighed with respect to each individual opening area (m),
- $A_t$  = total interior area of the surfaces bounding the compartment, opening areas included ( $\text{m}^2$ ),
- $m_v$  = total weight of combustible material  $v$  (kg)
- $H_v$  = effective heat value of combustible material  $v$  of the fire load ( $\text{MJ} \cdot \text{kg}^{-1}$ ), and
- $\mu_v$  = a fraction between 0 and 1, giving the real degree of combustion for each individual component of the fire load.

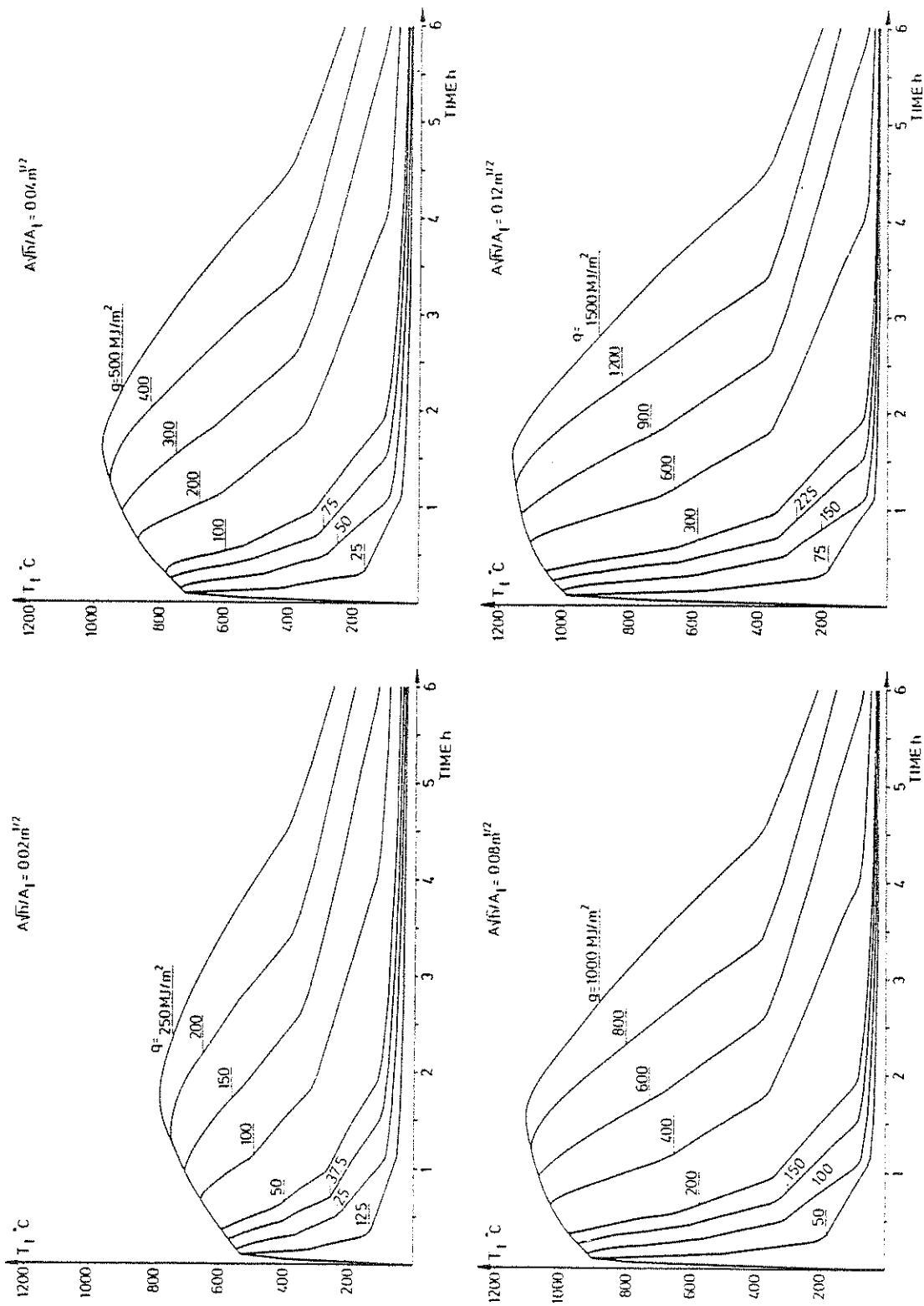


Figure 11. Gas temperature-time curves  $T_t$ - $t$  of the complete process of fire development for different values of the fire load density  $q$  and the opening factor  $A_f h / A_t$ . Fire compartment, type A



The non-dimensional factor  $\mu_v$  is a function of type of fuel, geometrical properties of fuel, and the position of fuel in a fire compartment, among other things. For some types of fire load components,  $\mu_v$  will depend on the time of fire duration and on the gas temperature-time characteristics of the fire compartment. Bookcases and floor coverings are examples of fire components whose real degree of combustion is low, and whose  $\mu_v$  values are probably appreciably below unity. At present, however, there is a lack of experimentally substantiated and verified  $\mu_v$  values, and it is therefore usually necessary in the course of practical design to employ a fire load calculation with  $\mu_v$  generally put equal to unity.

As a rule, the design fire load density is to be determined on the basis of statistical investigations for the type of building or premises in question. Such statistical investigations have been carried out for dwellings, offices, administration buildings, schools, stores, and hospitals [2], [4], [6]. As a temporary regulation, the Swedish Building Code authorizes the 80 percent level of the statistical distribution curve to be applied as the design fire load density.

A fragmentary example of the results, obtained in the statistical investigations of the fire load density  $q$ , is given in Fig. 12 [20], which refers some distribution curves, representative to dwellings in the suburbs and the central parts of Stockholm. In the figure the fire load density is specified on one hand by a minimum value, which only includes the highly inflammable components, and on the other hand by a maximum value, corresponding to all combustible material in the compartment, excluding floor covering. Table A1 in the appendix summarizes the average and standard deviation of the fire load density as well as the design fire load density from the investigations, determined according to Eq. (3) with  $\mu_v = 1$  [2], [4], [6].

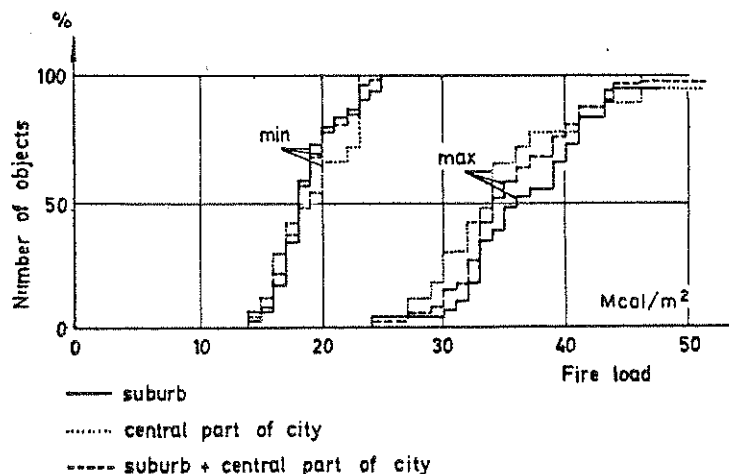


Figure 12. Distribution curves for the fire load density  $q$ , defined according to Eq. (3), representative to dwellings in the suburbs and the central parts of Stockholm.  $1 \text{ Mcal/m}^2 = 4.19 \text{ MJ/m}^2$

The gas temperature-time curves in Fig. 11 have generally been determined on the assumption of ventilation controlled fires. For fires, which are fuel bed controlled in reality, this assumption leads to a structural fire engineering design on the safe side in practically every case, giving an overestimation of the maximum gastemperature and a simultaneous, partly balancing underestimation of the fire duration. For the minimum load-bearing capacity, which thermally can be seen as an integrated effect, the gas temperature-time curves in Fig. 11 give reasonably correct results, verified in [4], [10], [16].

As pointed out, the gas temperature-time curves in Fig. 11 apply to a certain fire compartment, type A, specified with respect to the thermal properties of its surrounding structures. Fire compartments with surrounding structures of deviating thermal properties can be transferred to fire compartment, type A, via effective values of the fire load density  $q_f$  and the opening factor  $(A\sqrt{h}/A_t)_f$  in accordance to Table A2 in the appendix [2], [4], [6].

### 3.2 Opening Factor $A\sqrt{h}/A_t$

According to Fig. 11, the opening factor of a fire compartment is a fundamental concept in calculating the gastemperature-time curve of the process of fire development.

For a fire compartment with only vertical openings, the opening factor is defined by the quantity  $A\sqrt{h}/A_t$ , where - cf. Fig. 13

- A = total area of the window and door openings ( $m^2$ ),
- h = mean value of the heights of window and door openings (m), weighed with respect to each individual opening area, and
- $A_t$  = total interior area of the surfaces bounding the compartment, opening areas included ( $m^2$ ).

If a fire compartment also comprises horizontal openings, an equivalent opening factor  $(A\sqrt{h}/A_t)_e$  can be determined by the formula [15]

$$(A\sqrt{h}/A_t)_e = f_k (A\sqrt{h}/A_t)_v \quad (4)$$

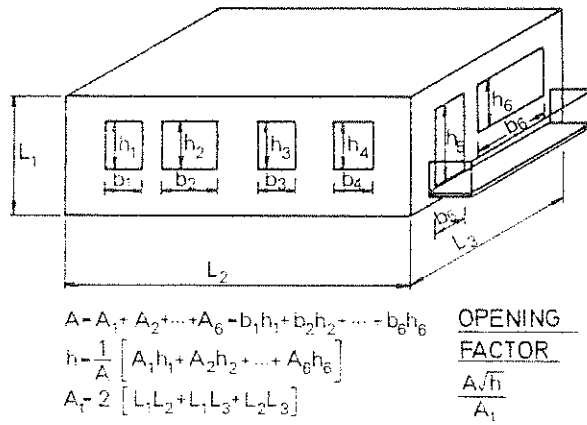


Figure 13. Definitions of the total opening area  $A$ , the weighed mean value of the opening height  $h$ , the total interior area of the surrounding structures  $A_t$ , and the opening factor  $A\sqrt{h}/A_t$  of a fire compartment

where  $(A\sqrt{h}/A_t)_v$  is the opening factor, corresponding to the vertical openings of the compartment, calculated according to Fig. 13, and  $f_k$  a dimensionless multiplier, given by the alignment chart in Fig. 14. For the notations used in this chart, then see Fig. 15.

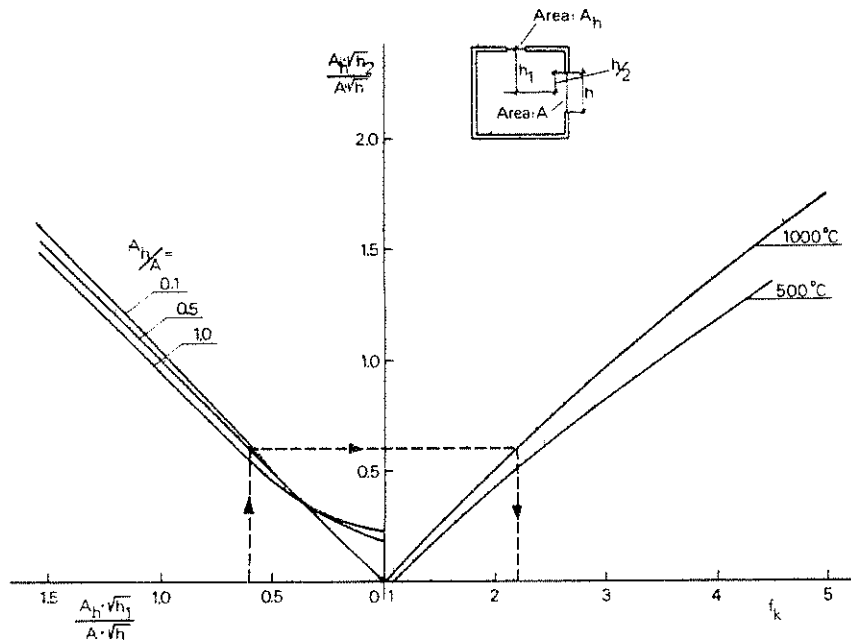


Figure 14. Alignment chart for a determination of the equivalent opening factor  $(A\sqrt{h}/A_t)_e$  of a fire compartment with vertical as well as horizontal openings. For notations, see Fig. 15

A determination of the equivalent opening factor over Eq. (4) and Fig. 14 presupposes that the gas flow through the horizontal openings of the roof is not predominant. This can be examined via the quotient  $A_h \sqrt{h_2}/A \sqrt{h}$ , which has an upper limit at which the applied gas flow model ceases to be valid. This upper limit is given by the values



- $\Delta T_s$  = change of steel temperature ( $^{\circ}\text{C}$ ) during time step  $\Delta t(\text{s})$ ,  
 $\alpha$  = coefficient of heat transfer at fire exposed surface of structure ( $\text{W}\cdot\text{m}^{-2}\cdot^{\circ}\text{C}^{-1}$ ),  
 $\rho_s$  = density of steel material ( $7850 \text{ kg}\cdot\text{m}^{-3}$ ),  
 $c_{ps}$  = specific heat of steel material ( $\text{J}\cdot\text{kg}^{-1}\cdot^{\circ}\text{C}^{-1}$ ),  
 $F_s$  = fire exposed surface of steel structure per unit length (m),  
 $V_s$  = volume of steel structure per unit length ( $\text{m}^2$ ),  
 $T_t$  = gas temperature ( $^{\circ}\text{C}$ ) within fire compartment at time  $t$  (s).

Eq. (6) presupposes that the steel temperature  $T_s$  is uniformly distributed over the cross section of the structure at any time  $t$ .

The coefficient of heat transfer  $\alpha$  can be calculated from the approximate formula

$$\alpha = 23 + \frac{5.77 \epsilon_r}{T_t - T_s} \left[ \left( \frac{T_t + 273}{100} \right)^4 - \left( \frac{T_s + 273}{100} \right)^4 \right] \quad (\text{W}\cdot\text{m}^{-2}\cdot^{\circ}\text{C}^{-1}) \quad (7)$$

giving an accuracy which is sufficient for ordinary practical purposes.  $\epsilon_r$  is the resultant emissivity which for practical applications can be chosen according to the following table, giving values which generally are on the safe side.

1. Column, fire exposed on all sides	$\epsilon_r = 0.7$
2. Column, outside a facade	0.3
3. Floor structure, composed of steel beams with a concrete slab on the lower flange of the beams	0.5
4. Steel beams with a floor slab on the upper flange of the beams	
4a. Beams of I cross section with width/height $\geq 0.5$	0.5
4b. Beams of I cross section with width/height $< 0.5$	0.7
4c. Beams of box cross section and trusses	0.7

More accurate values of the resultant emissivity  $\epsilon_r$  can be determined for the application alternative 4 - steel beams with a floor slab, supported on the upper flange of the beams - from the diagrams of Fig. 17 and 18, applicable to floor structures with the flames completely below the steel beams and reaching the slab, respectively [22]. For the emissivity of the

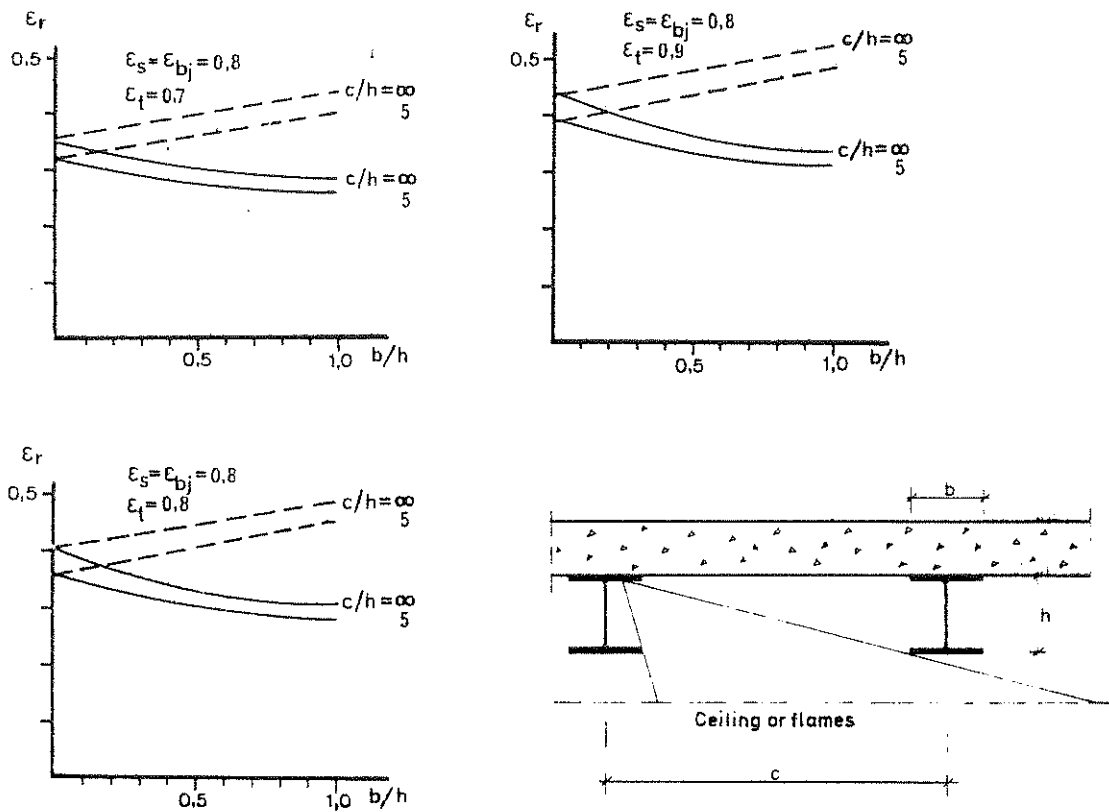


Figure 17. Resultant emissivity  $\epsilon_r$  for steel beams with a floor slab, supported on the upper flange of the beams. Flames completely below the steel beams.

$\epsilon_{bj}$  = emissivity of the slab,  $\epsilon_s$  = emissivity of the steel beams,  $\epsilon_t$  = emissivity of the flames.

— I cross section, ---- box cross section

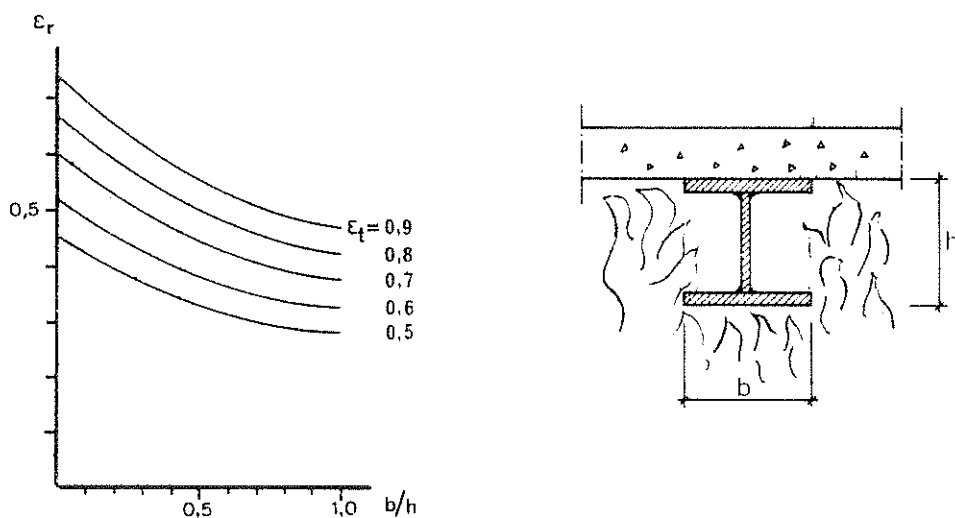


Figure 18. Resultant emissivity  $\epsilon_r$  for steel beams of I cross section with a floor slab, supported on the upper flange of the beams. Flames reaching the slab.

$\epsilon_t$  = emissivity of the flames

flames  $\epsilon_t$ , the value 0.85 is to be inserted, if not any other value can be proved to be more correct.

At a given gas temperature-time curve  $T_t-t$  of the fire compartment, the steel temperature  $T_s$  can be directly calculated from Eqs. (6) and (7) with regard taken to the temperature dependence of  $c_{ps}$  and  $\alpha$ . Such computations have been carried out in a systematized way, giving the basis of design in Table A3 in the appendix [4]. From this table, the maximum steel temperature  $T_{s,max}$  during a complete compartment fire can be determined directly as a function of the effective fire load density  $q_f$ , the effective opening factor  $(A\sqrt{h}/A_t)_f$ , the  $F_s/V_s$  ratio and the resultant emissivity  $\epsilon_r$ . The values of the table are connected to gas temperature characteristics according to Fig. 11.

Table A4 in the appendix gives some guide-lines for the determination of the structural parameter  $F_s/V_s$  for different types of application.

### 3.4 Design Temperature State of Fire Exposed, Insulated Steel Structures

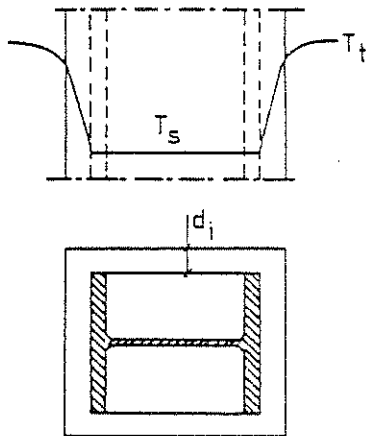


Figure 19. Fire exposed, insulated steel structure.  $T_t$  = gas temperature within fire compartment,  $T_s$  = steel temperature at time  $t$

For a fire exposed, insulated steel structure, a simplified energy balance equation gives the following formula for a direct determination of the steel temperature-time curve  $T_s-t$  - Fig. 19

$$\Delta T_s = \frac{A_i}{(1/\alpha + d_i/\lambda_i)\rho_s c_{ps} V_s} (T_t - T_s)\Delta t \quad (^\circ\text{C}) \quad (8)$$

with the additional quantities

$A_i$  = interior jacket surface area of insulation per unit length (m),

$d_i$  = thickness of insulation (m),

$\lambda_i$  = thermal conductivity of insulating material ( $\text{W}\cdot\text{m}^{-1}\cdot^\circ\text{C}^{-1}$ ).



Eq. (8) presupposes that the steel temperature  $T_s$  is uniformly distributed over the cross section of the structure at any time  $t$ , that the temperature gradient is linear and the heating contribution negligible for the insulation, and that the heat transfer is one-dimensional.

Computations, originating from Eqs. (7) and (8), enable a production of a systematized design basis, facilitating an analytical, differentiated fire engineering design in practice. An example from such a design basis is referred in Table A5 in the appendix [4], giving the maximum steel temperature  $T_{s,max}$  during a complete compartment fire for varying values of the effective fire load density  $q_f$ , the effective opening factor  $(A\sqrt{h}/A_t)_f$ , the structural parameter  $A_i/V_s$ , and the insulation parameter  $d_i/\lambda_i$ . The values of the table are connected to gas temperature characteristics according to Fig. 11.

Table A5 was computed on the assumption of a constant thermal conductivity of the insulating material  $\lambda_i$ , chosen as an average value for the whole compartment fire process. Calculations, carried through systematically, are verifying that this average value of  $\lambda_i$  approximately coincides with the value, determined for an insulation temperature equal to the maximum steel temperature  $T_{s,max}$ . Table A6 in the appendix gives the thermal conductivity  $\lambda_i$  of some insulation materials as a function of the temperature [4].

For a specific insulating material, systematized design diagrams or tables can be computed very accurately with regard to the temperature dependence of the thermal properties of the steel as well as the insulating material. The influence of an initial moisture content and of a disintegration of the insulating material can be considered, too. Practically, such a determination can be carried out over a numerical data processing by computers on the basis of a finite difference or a finite element method. A great number of design tables, computed according to such an accurate procedure, are presented in [4]. Table A7 in the appendix exemplifies this, giving the maximum steel temperature  $T_{s,max}$  at varying fire and structural design characteristics for a fire exposed steel structure, insulated with mineral wool of density  $\rho_i = 150 \text{ kg m}^{-3}$  at varying effective fire load density  $q_f$ , effective opening factor  $(A\sqrt{h}/A_t)_f$ , quotient  $A_i/V_s$ , and thickness  $d_i$  of the insulation.

Table A8 in the appendix gives some guide-lines for the determination of the structural parameter  $A_i/V_s$  for different types of application.

### 3.5 Design Temperature State of Fire Exposed Floor or Roof Assembly with Suspended Ceiling

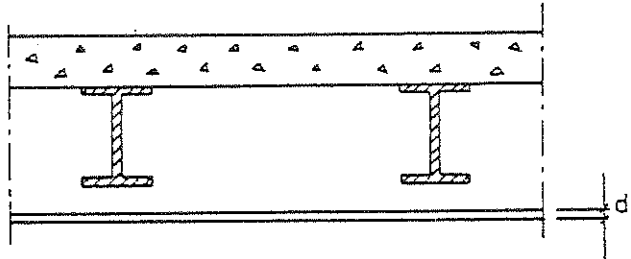


Figure 20. Floor structure, composed of a reinforced concrete slab, load-bearing steel beams, and an insulating ceiling

In [4], an analytical model is derived for a simplified determination of the temperature-time fields of a steel beam structure according to Fig. 20 - composed of a reinforced concrete slab, load-bearing steel beams, and an insulating ceiling - exposed to a fire from below. By applying this computational model in a systematic way, a design basis has been determined, facilitating a calculation of the steel beam temperature  $T_s$ , assumed as uniformly distributed over the cross section of the beams. The design basis is exemplified in Table A9 in the appendix [4], which gives the maximum steel beam temperature  $T_{s,max}$  during a complete compartment fire for varying values of the effective fire load density  $q_f$ , the effective opening factor  $(A\sqrt{h}/A_t)_f$ , the structural parameter  $F_s/V_s$ , and the insulation parameter  $d_i/\lambda_i$ .  $F_s$  denotes the surface area of the steel beam, less the part covered by the concrete slab, and  $V_s$  the volume of the steel beam, per unit length. The values, given in brackets in the table, denote the corresponding maximum temperature at the centre level of the ceiling. The values of the table are connected to gas temperature characteristics according to Fig. 11.

For several types of steel beam structures with a suspended, insulating ceiling, the fire resistance of the ceiling and its fastening devices will be the decisive design criterion instead of the temperature of the steel beams. The ceiling can get a serious crack formation or fall down, partially or completely, after a comparatively short fire exposure. Under such conditions, the maximum steel beam temperature

cannot be determined from Table A9 solely on the basis of the thickness  $d_i$  and the thermal conductivity  $\lambda_i$  of the ceiling. If results are available for a type of a suspended ceiling from a standard fire resistance test, these results can be used for deriving an effective value of the insulation parameter  $d_i/\lambda_i = (d_i/\lambda_i)_{\text{eff}}$  - which describes the real fire behaviour of the suspended ceiling, including its fastening devices. From the test results, also a possible critical failure temperature of the suspended ceiling can be estimated. Cf., further [4].

After the determination of  $(d_i/\lambda_i)_{\text{eff}}$  and the critical temperature of a type of a suspended ceiling, the analytical differentiated fire design can be carried out by a direct application of Table A9. Parallely, then the maximum temperature at the centre level of the ceiling according to the table must be controlled against the critical temperature of the ceiling.

Effective  $d_i/\lambda_i$  values and critical temperatures have been determined for a number of types of suspended ceilings in a series of standard fire resistance tests performed at the National Swedish Institute for Testing and Metrology in Stockholm [23]. The compositions of these suspended ceilings, the results obtained and the characteristics derived are set out in Table A10 in the appendix [4].

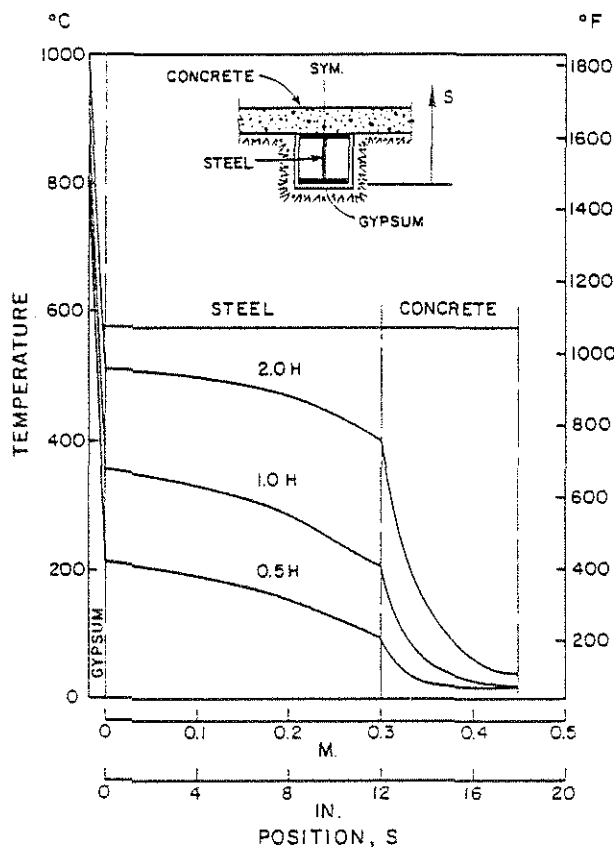


Figure 21. Calculated temperature distribution along line of symmetry of a steel beam, insulated by a 16 mm gypsum board (density  $770 \text{ kg}\cdot\text{m}^{-3}$ ) and carrying a 150 mm concrete slab on top flange, at selected times of a thermal exposure according to ISO 834 [24]

The design basis, reproduced in Tables A3, A5, A7 and A9, generally assumes the steel temperature to be uniformly distributed over the cross section of the beam or column at any time  $t$ . A more accurate theory, which enables a determination of the temperature variation over the cross section of the steel structure, is presented in [24], together with computer routines. The algorithm described can easily be coupled to most finite element programs. An illustration of the capability of the theory is given in Fig. 21, which shows calculated temperature distribution along the line of symmetry of a gypsum insulated steel beam with a concrete slab at the top flange at selected times of a standard fire resistance test according to ISO 834.

### 3.6 Design Temperature State of Fire Exposed Partitions

As a complement to the design temperature state of fire exposed load-bearing steel structures, dealt with above, also some remarks will be given on the fire engineering design of partitions. The performance requirements for partitions imply that these must prevent a penetration of flames and hot gases and limit the rise in temperature on the unexposed side of the construction during a complete compartment fire.

An analytical method for a determination of the temperature-time field in a multi-layer partition is presented in [25]; cf. also [4]. The method considers the temperature dependence of the thermal material properties, an initial moisture content, and a possible material disintegration at specified temperature criteria. An illustrating application of the method is shown in Fig. 22 [25], which gives a summary conception of the fire behaviour of a steel stud wall, insulated on each side with two 13 mm gypsum plaster sheets, type Gyproc, of density  $790 \text{ kg}\cdot\text{m}^{-3}$ , fire exposed on one side and acting as a partition. The behaviour has been determined on the basis of temperature dependent thermal properties of gypsum plaster material according to Fig. 23 and a critical failure temperature for a gypsum plaster sheet of  $550^\circ\text{C}$  on that side of the sheet facing away from the fire. The results of full scale fire tests confirm this failure criterion.

Fig. 22a describes the fire behaviour of the wall, when it is fire exposed on one side by a compartment fire with gas temperature-time

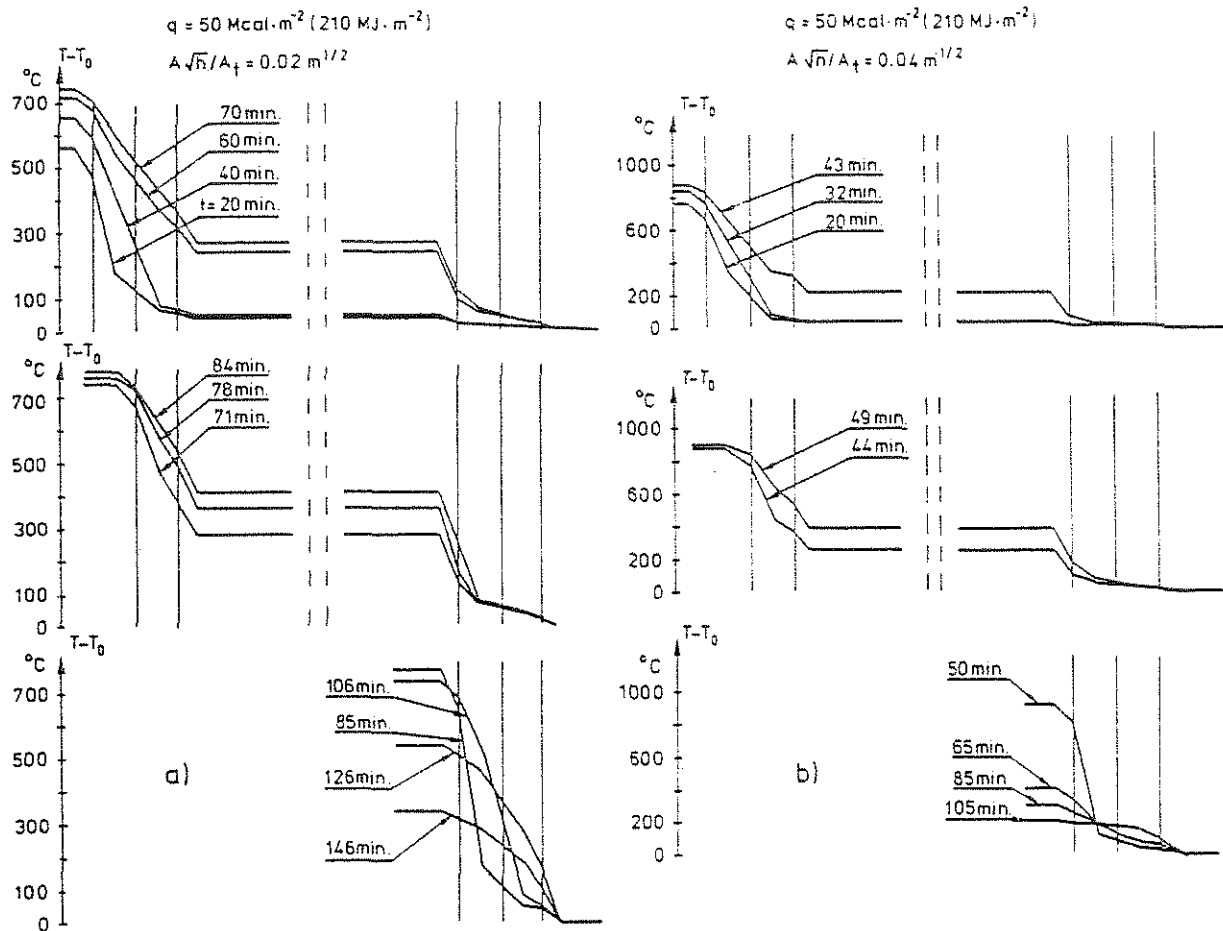


Figure 22. Calculated temperature-time fields for a steel stud wall, insulated on each side with two 13 mm gypsum plaster sheets, type Gyproc, of density  $790 \text{ kg} \cdot \text{m}^{-3}$ . The wall is fire exposed on one side with compartment fire characteristics according to Fig. 11: a)  $q = 50 \text{ Mcal} \cdot \text{m}^{-2}$  ( $210 \text{ MJ} \cdot \text{m}^{-2}$ ),  $A\sqrt{h}/A_t = 0.02 \text{ m}^{1/2}$ ; b)  $q = 50 \text{ Mcal} \cdot \text{m}^{-2}$  ( $210 \text{ MJ} \cdot \text{m}^{-2}$ ),  $A\sqrt{h}/A_t = 0.04 \text{ m}^{1/2}$ .  $T_0$  = temperature at time  $t = 0$  [25]

characteristics according to Fig. 11 - fire load density  $q = 50 \text{ Mcal} \cdot \text{m}^{-2}$  ( $210 \text{ MJ} \cdot \text{m}^{-2}$ ), opening factor  $A\sqrt{h}/A_t = 0.02 \text{ m}^{1/2}$ . The figure gives a calculated failure of the directly fire exposed gypsum plaster sheet after about 70 min and of the next gypsum plaster sheet after about 85 min. The maximum temperature rise on the unexposed side of the wall amounts to  $180^\circ\text{C}$  during the complete fire process, i.e. precisely the maximum permissible value according to [2]. Fig. 22b analogously describes the fire behaviour of the wall, when it is exposed to a more rapid compartment fire - opening factor  $A\sqrt{h}/A_t = 0.04 \text{ m}^{1/2}$  - at the same fire load density  $q$ . The increase of the opening factor results in a considerably decreased value of the maximum temperature rise on the unexposed side of the wall, which amounts to only about  $55^\circ\text{C}$  in this case.

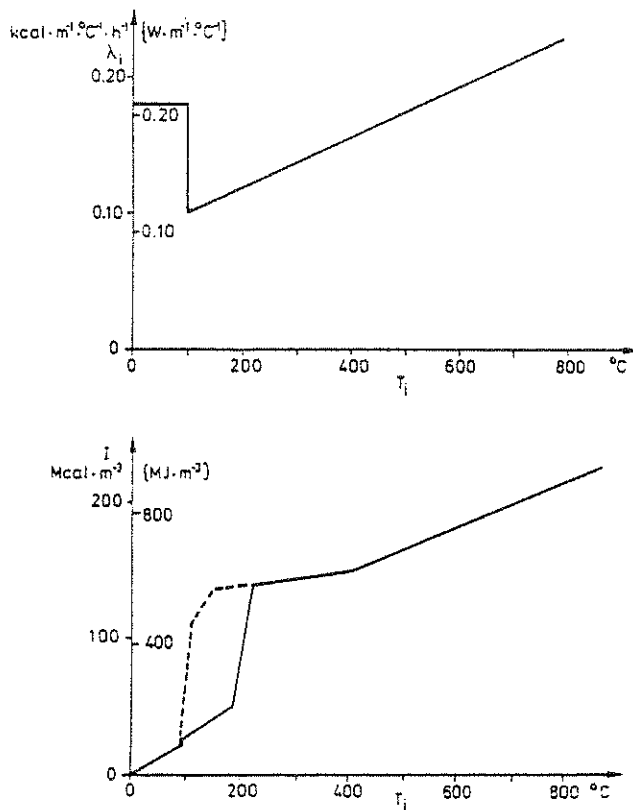


Figure 23. Thermal conductivity  $\lambda_i$  and enthalpy  $I (= \int_0^T c_p dT)$  as a function of insulation temperature  $T_i$  for gypsum plaster slabs, type Gyproc, of density  $790 \text{ kg} \cdot \text{m}^{-3}$ . For enthalpy  $I$ , full line refers to a rapid heating and dashed line to a slow heating [25], [26]

Systematic calculations of the type, illustrated by Fig. 22, lead to design diagrams as shown in Fig. 24 [4], [6], giving the maximum temperature  $T_{v,\max}$  during a complete fire process on the unexposed side of a steel stud-gypsum plaster sheeting wall as a function of the effective fire load density  $q_f$  and the effective opening factor of the fire compartment  $(A\sqrt{h}/A_t)_f$ . The two diagrams apply to an insulation on each side of the wall with one and two 13 mm gypsum plaster sheets, type Gyproc, of density  $790 \text{ kg} \cdot \text{m}^{-3}$ , respectively. The calculated  $T_{v,\max}$  values are to be compared with the corresponding maximum temperature, permitted in the Swedish Building Code, which implies  $200^{\circ}\text{C}$  as an average temperature and  $240^{\circ}\text{C}$  as a temperature over limited areas of the unexposed side of the partition [2].

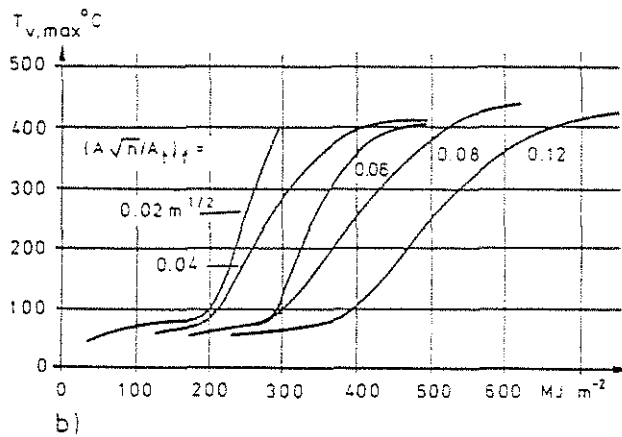
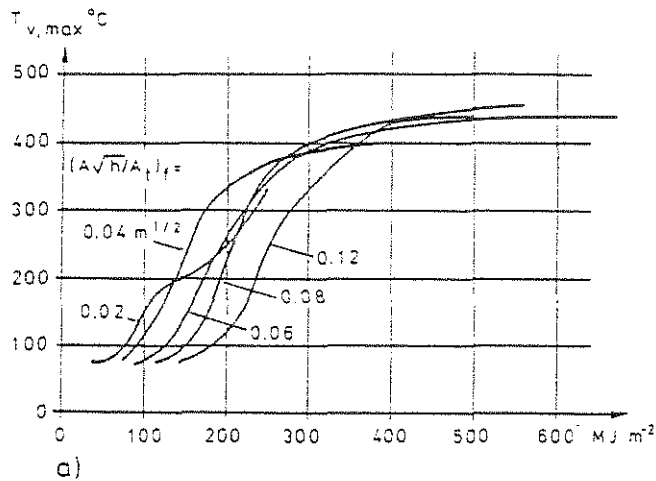


Figure 24. Maximum temperature  $T_{v,max}$  during a complete fire process according to Fig. 6 on the unexposed side of a steel-gypsum plaster sheeting wall as a function of the effective fire load density  $q_f$  and the effective opening factor  $(A\sqrt{h}/A_f)_f$  of the fire compartment. The wall is insulated on each side with one (fig a) or two (fig b) 13 mm gypsum plaster sheets, type Gyproc, of density  $790 \text{ kg}\cdot\text{m}^{-3}$  [4], [6]

### 3.7 Design Load Effect and Design Load-Bearing Capacity of Fire Exposed Steel Structures

In the design, it is to be proved that the design load-bearing capacity of the fire exposed structure does not decrease below the design load effect during the complete process of fire development. The design load effect then is to be chosen on the basis of the most unfavourable combination of dead load, live load, snow load and wind load.

Table A11 in the appendix refers the load values, specified in the Swedish Building Code for a differentiated, analytical, structural fire engineering design [2], [4], [6]. The specified load values are differentiated with respect to whether a complete evacuation of people can be



assumed or not in the event of fire. The values include a safety factor which roughly considers the probability of a fully developed fire and the probability of the presence of the maximum load at the fire occasion.

By applying the design tables A3 to A10, the maximum steel temperature  $T_{s,max}$  can be determined comparatively quickly for an uninsulated or insulated steel structure, exposed to a complete compartment fire with gas temperature-time characteristics according to Fig. 11. The corresponding design load-bearing capacity of the structure then is obtained by design diagrams of the type exemplified in Fig. 25, 26 and 27.

Fig. 25 and 26 [4], [6] give the design load-bearing capacity ( $M_{cr}$ ,  $P_{cr}$ ,  $q_{cr}$ ) of fire exposed beams of constant I cross section at different types of loading and support conditions, as a function of the steel beam temperature  $T_s$ . The design curves in Fig. 25 apply to a slow rate of heating - assumed to be  $4^{\circ}\text{C}\cdot\text{min}^{-1}$ , followed by a cooling with a rate of  $1.33^{\circ}\text{C}\cdot\text{min}^{-1}$  - and Fig. 26 gives the correction  $\Delta\beta$  of the load-bearing capacity coefficient  $\beta$  due to a more rapid rate of heating. In the formulas for the load-bearing capacity

$\sigma_s$  = yield stress of steel material at room temperature (MPa),  
 $L$  = span of beam (m),  
 $W$  = elastic modulus of beam cross section ( $\text{m}^3$ ).

The design curves in Fig. 25 and 26 have been determined on the basis of the deformation curve of the fire exposed beams calculated by an analytical model, presented in [27], which takes into account the softly rounded shape of the stress-strain curve of steel at elevated temperatures as well as the influence of creep strain. As can be seen from Fig. 26, this influence of creep begins to be noticeable for ordinary structural steels at temperatures in excess of about  $450^{\circ}\text{C}$ . The load-bearing capacity of the beams is defined by the limit deflection criterion according to ROBERTSON and RYAN [28].

The diagrams in Fig. 27 [4] determine the variation with the steel temperature  $T_s$  of the relationship between the buckling stress  $\sigma_{cr}$  and the slenderness ratio  $\lambda$  for fire exposed columns, axially loaded in compression. The diagrams apply to steel having a yield stress at room temperature  $\sigma_s = 220, 260$  and  $320$  MPa, respectively, and are valid under the

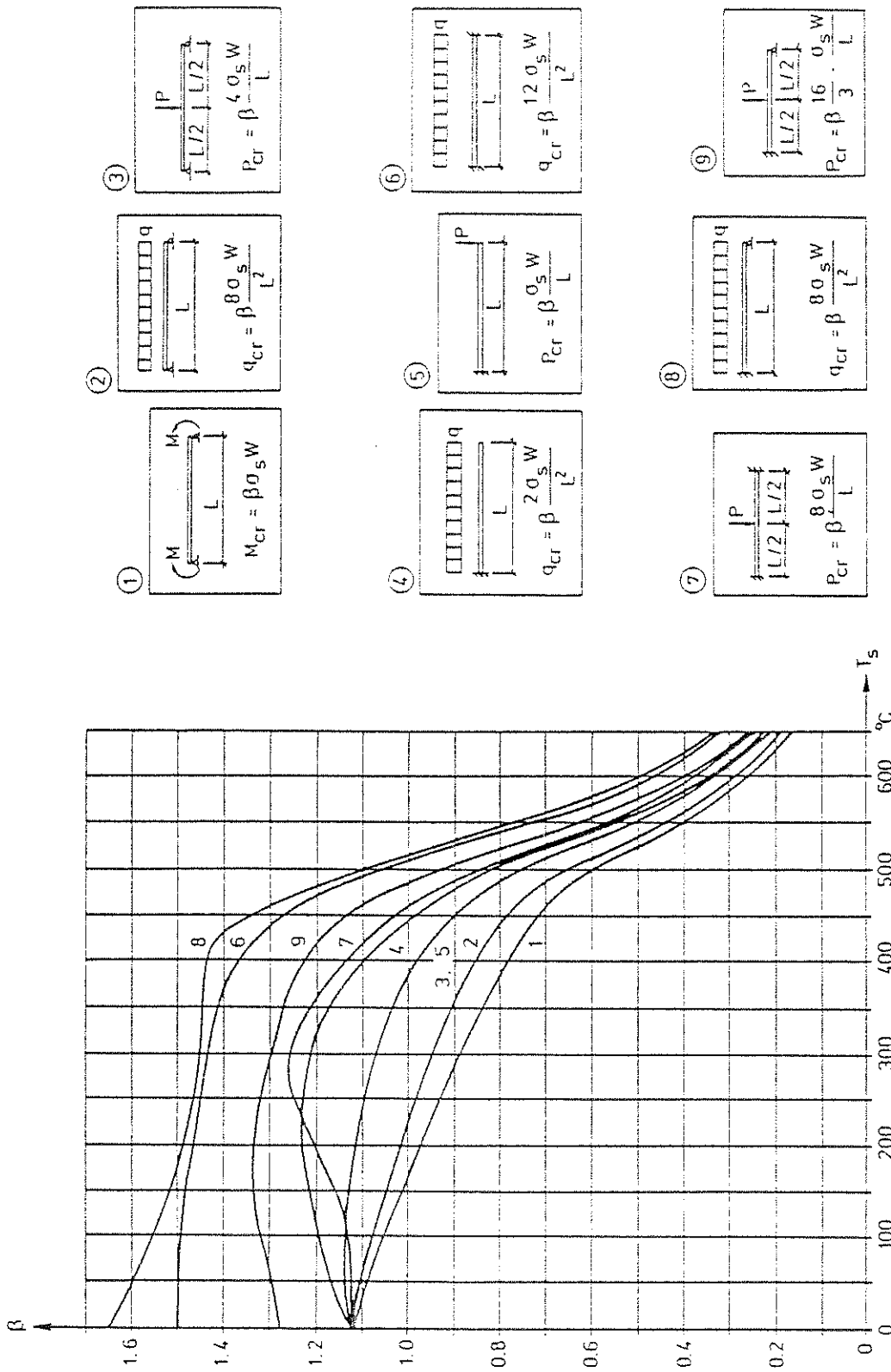


Figure 25. Coefficient  $\beta$  for determination of critical load ( $M_{cr}$ ,  $P_{cr}$ ,  $q_{cr}$ ) for fire exposed beams of I cross section at different types of loading and support conditions, as a function of the steel beam temperature  $T_s$ . The curves have been calculated for a slow rate of heating of  $4^{\circ}\text{C}\cdot\text{min}^{-1}$  and a subsequent cooling, assumed to be one third of the rate of heating [4], [6]

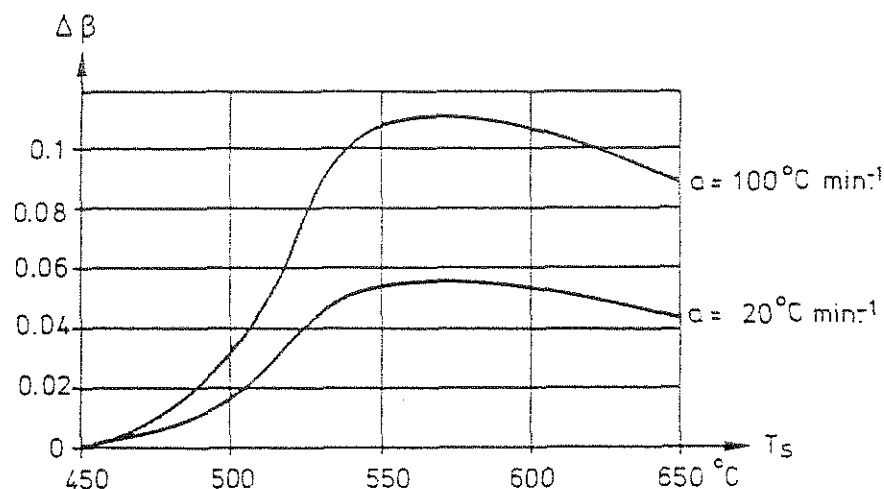


Figure 26 . Increase  $\Delta\beta$  of coefficient  $\beta$ , determined according to Fig. 25, for a rate of heating  $\alpha \geq 4^\circ\text{C}\cdot\text{min}^{-1}$ , as a function of the steel beam temperature  $T_s$  [4], [6]

presumption that the column is unrestrained with respect to longitudinal expansion during the fire exposure. The  $\sigma_{cr}-\lambda$  curves have been computed for an initially deflected and excentrically loaded column on the basis of data on the change of the 0.5 % proof stress  $\sigma_{0.5}$  and the secant modulus with the temperature, obtained in tension tests at a very slow rate of loading. This implies that a considerable influence of short-time creep at elevated temperatures is included.

For a fire engineering design of columns, partly restrained to a longitudinal expansion, reference is made to [4].

The design curves, reproduced in Fig. 25, 26 and 27, are generally based on the assumption of a uniformly distributed temperature over the cross section of the steel structure at any time  $t$  during the fire exposure. By this assumption, the design curves are directly connected to Tables A3, A5, A7 and A9, determining the design temperature state of the steel structure.

If the analytical, differentiated design of fire exposed steel structures will be further developed in future towards a more accurate determination of the design temperature state, with regard taken to the temperature variation over the cross section of the steel structure, this will also require a more refined basis of design for the transfer of the design temperature state to the design load-bearing capacity of the fire exposed structure. The first attempts of developing such a more refined design

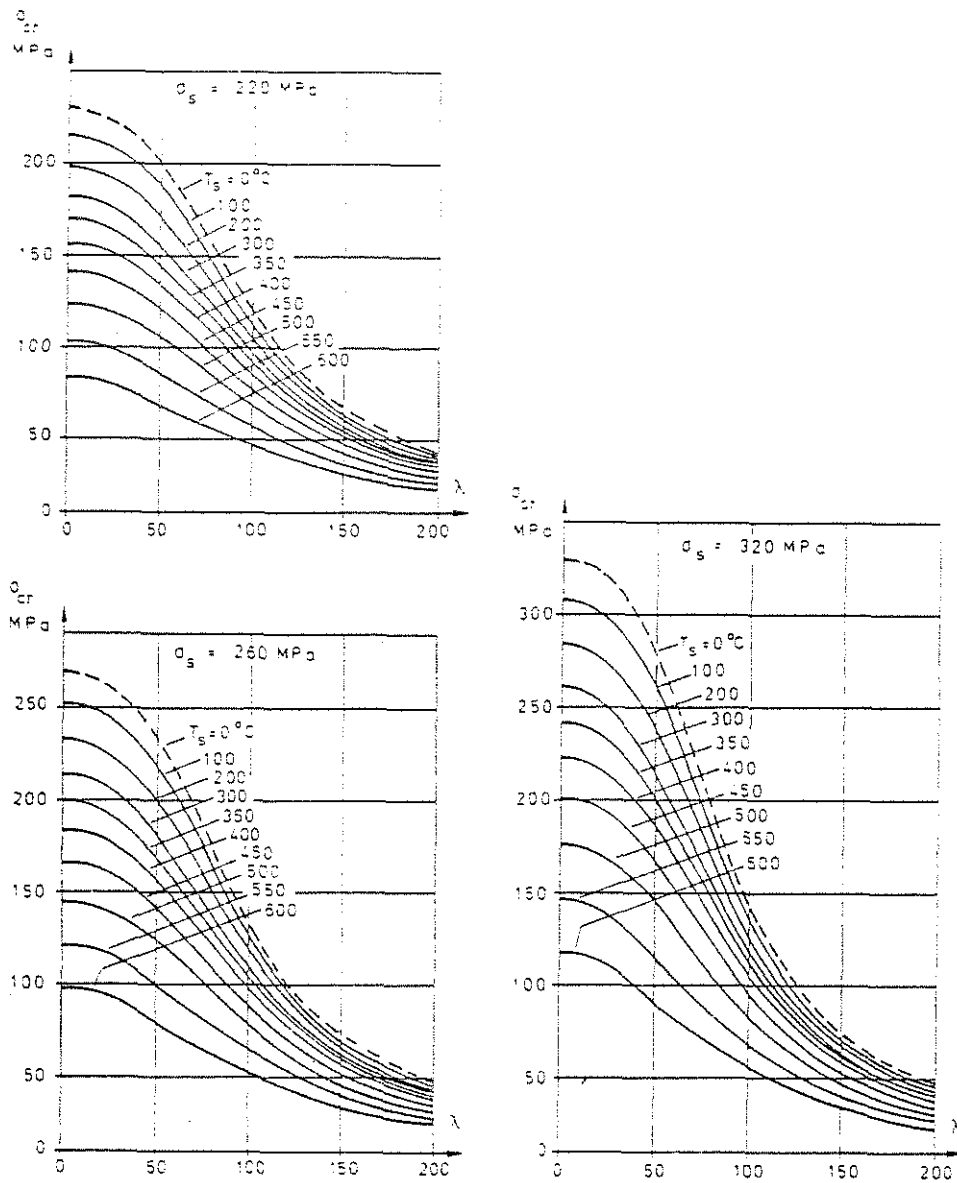


Figure 27. Variation with steel temperature  $T_s$  of the relationship between buckling stress  $\sigma_{cr}$  and slenderness ratio  $\lambda$  for fire exposed steel columns, axially loaded in compression, free to expand longitudinally and made of steel having a yield stress at room temperature  $\sigma_s = 220$ , 260 and 320 MPa, respectively [4], [6]

basis now can be noticed in the literature. As a fragmentary example of this development, Fig. 28 [29] shows the calculated variation of the plastic bending moment of a fire exposed steel I cross section as a function of the maximum temperature for various linear temperature distributions over the cross section.

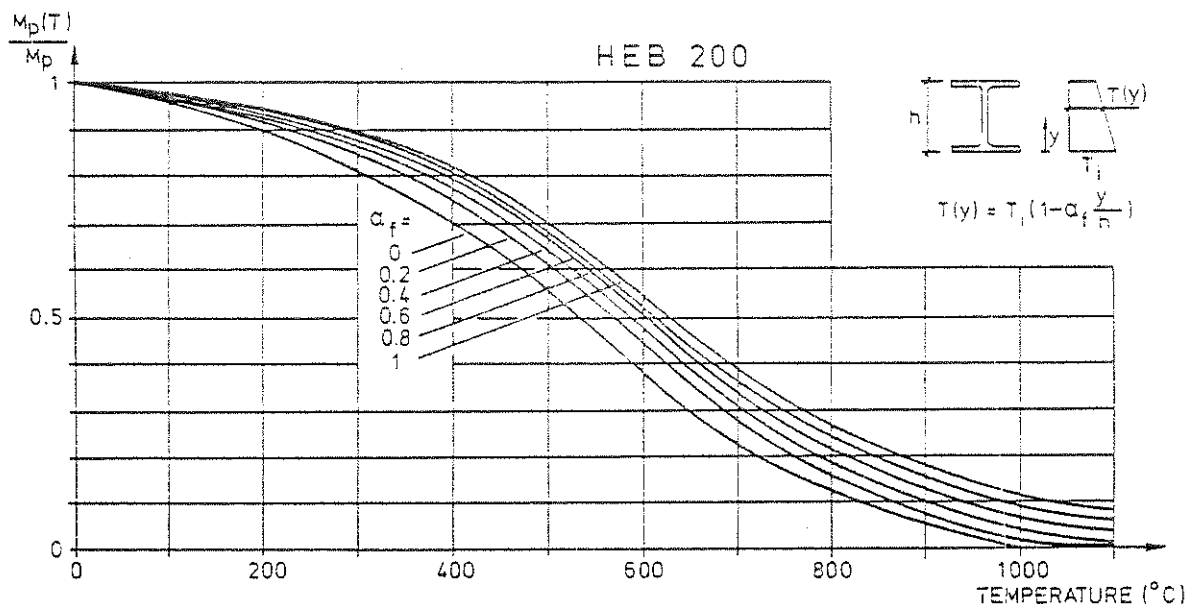


Figure 28. Calculated variation of plastic bending moment  $M_p(T)$  in terms of various linear temperature distribution over height of a steel I cross section [29]

#### 4. Concluding Remarks

A differentiated procedure is presented for an analytical fire engineering design of load-bearing steel structures and partitions. The procedure is a direct design method based on gas temperature-time characteristics of a complete compartment fire, which depends on the fire load density, the ventilation of the fire compartment and the thermal properties of the structures enclosing the fire compartment. The practical use for the design procedure has been approved by the National Swedish Board of Physical Planning and Building.

For the practical application of the design procedure, a comprehensive design basis in the form of diagrams and tables has been worked out for a direct determination of the maximum steel temperature during a complete compartment fire and the corresponding design load-bearing capacity of the fire exposed structure. Included in this paper is also a worked out example, providing a rough impression of the more important features of the methodology.

Compared with the conventional fire engineering design, based on classification and results of standard fire resistance tests, the presented analytical design procedure has a more logical structure, based on well-defined functional requirements and performance criteria. Of the ensuing advantages, the following are seen to be the main ones:

1. More consistent safety levels. This point has been elaborated in chapter 2.
2. Better economy. The cost of structural fire protection is, as a rule, hard to itemize and the cost - saving consequences have been quantified only in a few cases. Rough estimates indicate that while the cost for conventional structural fire protection may exceed 30 per cent of the cost for the steel frame material, the corresponding percentage may be as low as 10 with the design procedure based on analytical modelling, see Fig. 29. The latter figure is based on the assumption that the advantages are fully exploited of integrating the design of the structural steel fire protection into the overall design process (inner and outer walls are used as fire protection whenever possible, concrete floor slabs are placed on the lower flange of the girders, inherently providing a smaller area to insulate, etc.).

Finally, it is recognized that the design system presented is not homogeneous with respect to the present basis of knowledge for the different design steps. Naturally, this can be put forward as a criticism of the system. However, such a remark is not essential. Instead, this fact ought to be used as an important guide on how to systematize a future research work for making possible a successive improvement of the system.

### COSTS FOR FIRE PROTECTION

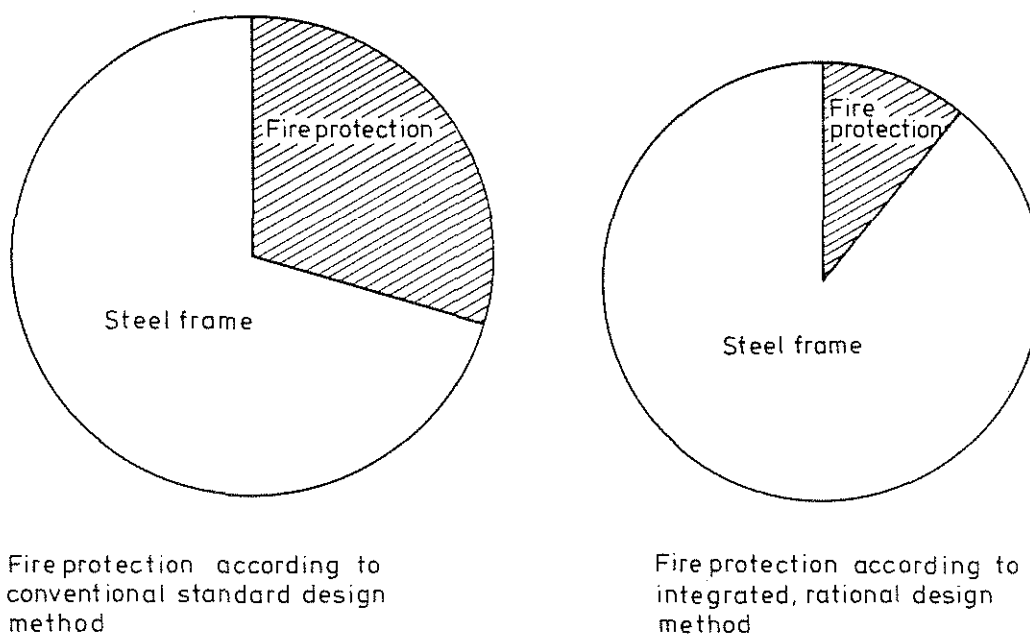


Figure 29.

## Example

### Introduction

The following example is solved in order to illustrate the practical application of the design procedure and to outline the computational scheme. The calculations may, for two reasons, seem somewhat lengthy and elaborate. Firstly, the problem to be solved has been chosen in order to include and emphasize several of the more important aspects of the design methodology. Secondly, for pedagogic reasons the calculations have been presented in a rather detailed manner. Several more worked out examples, giving a more balanced view of the practicality of the approach, may be found in Ref. 4.

### Background Data

A two-storey high school building is designed with a load-carrying steel frame of columns and simply supported girders according to Fig. 30. The material in columns and girders is steel quality 1412 with a nominal yield strength at room temperature  $\sigma_s = 260$  MPa.

The dimension of the center columns is HE 200 A and the girders in the floor-slab system are of size HE 280 B. Relevant data are given in Fig. 30. The center distance for girders and columns in the longitudinal direction of the building is 4 m.

The concrete floor assembly system is designed according to the figure. The dead weight of the system is  $7.0 \text{ kN m}^{-2}$ . The dead weight of the upper floor assembly system, including the weight of the roof, is  $7.0 \text{ kN m}^{-2}$ . The attic cannot be used for storage.

The fire compartment is defined by the materials in walls, floor and ceiling, by its geometric dimensions and the ventilation characteristics of door and windows. The horizontally bounding structures are the concrete slabs, inner walls are light-weight concrete with a density  $= 500 \text{ kg m}^{-3}$ . For the outer walls, two alternatives are to be studied

- alternative (a) sheet steel - mineral wool with density  $50 \text{ kg m}^{-3}$  - sheet steel
- (b) from inside 13 mm gypsum plaster board with density  $790 \text{ kg m}^{-3}$  - 100 mm mineral wool with density  $50 \text{ kg m}^{-3}$  - brick with density  $1800 \text{ kg m}^{-3}$

The task is to investigate if center columns and floor girders must be fire insulated. If so, determine the required insulation when using Unitherm fire retardant paint.

A design condition is that complete evacuation of the building in case of fire cannot be guaranteed.

### Step 1. Determination of the Design, Static Load

#### (a) Floor assembly girders

Dead weight of floor assembly system	7.0 kN m <sup>-2</sup>
Live load according to Table A11	0.5 + 1.5 = 2.0
Total, excluding dead weight of girders	9.0 kN m <sup>-2</sup>
Load per unit girder length, including estimated dead weight for girders	4 · 9.0 + 1.0 = 37 kN m <sup>-1</sup>

#### (b) Upper central column

Dead weight of upper ceiling assembly system, including roof	7.0 kN m <sup>-2</sup>
Snow load = normal design snow load 1 kN m <sup>-2</sup>	1.0
Total	8.0 kN m <sup>-2</sup>
Load per column = 7 · 4 · 8.0	224 kN
(Dead load of column neglected)	

#### (c) Lower central column

Dead weight of upper floor assembly system, including roof	7.0 kN m <sup>-2</sup>
Snow load as (b)	1.0
Dead weight of ceiling assembly system, including girders	7.3
Live load according to (a)	2.0
Total	17.3 kN m <sup>-2</sup>
Load per column (dead load of column neglected)	
7 · 4 · 17.3	484 kN

### Step 2. Determination of Effective Fire Load Density and Effective Ventilation Factor

The total bounding area of the fire compartment, including door and windows, is



$$A_t = 2L_1L_2 + 2L_1L_3 + 2L_2L_3 = 2 \cdot 2.5 \cdot 7.0 + 2 \cdot 2.5 \cdot 16.0 + 2 \cdot 7.0 \cdot 16.0 = 35.0 + 80.0 + 224.0 = 339 \text{ m}^2 \quad (\text{a})$$

Design fire load density for movable furnishings is given by Table A1,  $q_1 = 117 \text{ MJ m}^{-2}$ . To this must be added the fire load from the combustible flooring. The weight of the flooring is  $1.5 \text{ kg m}^{-2}$  with an effective calorific value  $= 21 \text{ MJ kg}^{-1}$ . This gives a contribution to the fire density =

$$q_{\text{floor}} = \frac{1.5 \cdot 21 \cdot 7 \cdot 16}{339} = 10 \text{ MJ m}^{-2}$$

Wall and ceiling lining materials are assumed incombustible. The total fire load density will be

$$q = q_1 + q_{\text{floor}} = 117 + 10 = 127 \text{ MJ m}^{-2} \quad (\text{b})$$

When determining the opening factor of the fire compartment, all window panes are assumed to be broken as a consequence of the fully developed fire. If the door is assumed closed and intact during the complete fire process, the opening factor will be

$$A = A_1 + A_2 + \dots = 1.5(5 \cdot 1.5 + 3.0) = 15.75 \text{ m}^2$$

$$h = 1.5 \text{ m}$$

$$\frac{A\sqrt{h}}{A_t} = \frac{15.75 \sqrt{1.5}}{339} = 0.0569 \text{ m}^{1/2} \quad (\text{c})$$

If the door is assumed open from outbreak of the fire, the opening factor equals

$$A = 15.75 + 0.9 \cdot 2.1 = 15.75 + 1.89 = 17.64 \text{ m}^2$$

$$h = \frac{\sum A_v h_v}{\sum A_v} = \frac{15.75 \cdot 1.5 + 1.89 \cdot 2.1}{17.64} = 1.56 \text{ m}$$

$$\frac{A\sqrt{h}}{A_t} = \frac{17.64 \sqrt{1.56}}{339} = 0.0650 \text{ m}^{1/2} \quad (\text{d})$$

The Tables A3 and A5, which give the relation between maximal steel temperature  $T_{s,\text{max}}$  and the combination of fire load density and opening

factor, indicate that the alternative with the lower opening factor value will give the higher steel temperature. Accordingly, the value of  $0.0569 \text{ m}^{1/2}$  for the opening factor will be chosen as basis for further calculations.

#### Effective Fire Load Density and Effective Opening Factor

The concept of effective fire load density  $q_f$  and effective opening factor  $(A\sqrt{h}/A_t)_f$  translates the values of fire load density and opening factor for the existing fire compartment to those of fire compartment type A, see Table A2. The purpose is to get an equivalent gastemperature-time curve from the number of curves computed for fire compartment type A and keep the volume of the design data base within reasonable limits.

#### Alternative (a)

Bounding structures of the fire compartment comprise the following material types and areas:

concrete floor assembly, area  $2.7 \cdot 16.0 = 224 \text{ m}^2$

inner walls of lightweight concrete, area  $\sim 2.5 \cdot 7.0 + 2.5 \cdot 16.0 = 57.5 \text{ m}^2$   
(door closed)

outer wall sheet steel - 100 mm mineral wool - sheet steel, area  
 $2.5 \cdot 7.0 + 2.5 \cdot 16.0 - 1.5 \cdot (5 \cdot 1.5 + 3.0) = 41.8 \text{ m}^2$

The relative proportions are 69, 18 and 13 percent respectively. The existing fire compartment can, with regard to thermal characteristics, be described as a combination of fire compartment type B (100 percent concrete), type C (100 percent light weight concrete) and type H (100 percent sheet steel with mineral wool insulation). The value of  $K_f$  is given by

$$K_f = \frac{69}{100}(K_f)_B + \frac{18}{100}(K_f)_C + \frac{13}{100}(K_f)_H = 0.69 \cdot 0.85 + 0.18 \cdot 3.0 + 0.13 \cdot 3.0 = 1.52$$

The fire compartment can also be seen as a combination of fire compartments B, D and H. In this case  $K_f$  will be given by

$$K_f = \frac{13}{100}(K_f)_H + \frac{18}{50}(K_f)_D + \frac{69-18}{100}(K_f)_B = 0.13 \cdot 3.0 + 0.36 \cdot 1.35 +$$

$$+ 0.51 \cdot 0.85 = 1.31 \quad (e)$$

These are the two possible alternatives to derive a  $K_f$ -value. According to the comments in Table A2 the lowest of the derived  $K_f$ -values is to be used in the further calculations. The effective values of fire load density  $q_f$  and opening factor  $(A\sqrt{h}/A_t)_f$  are now given by

$$q_f = K_f q = 1.31 \cdot 127 = 166 \text{ MJ m}^{-2} \quad (f)$$

$$(A\sqrt{h}/A_t)_f = K_f A\sqrt{h}/A_t = 1.31 \cdot 0.0569 = 0.0745 \text{ m}^{1/2} \quad (g)$$

#### Alternative (b)

In this alternative, the bounding structures comprise

concrete floor slab, area  $2 \cdot 7.0 \cdot 16.0 = 224 \text{ m}^2$

inner walls of lightweight concrete, area  $\sim 2.5 \cdot 7.0 + 2.5 \cdot 16.0 = 57.5 \text{ m}^2$

outer wall 13 mm gypsum plaster board with density  $790 \text{ kg m}^{-3}$  - 100 mm mineral wool with density  $50 \text{ kg m}^{-3}$  - brick with density  $1800 \text{ kg m}^{-3}$ , area =  $41.8 \text{ m}^2$ .

With regard to its thermal characteristics, the enclosure may be seen as a combination of fire compartments of type B, D and E. A linear interpolation will give as a result that fire compartment type D is to be included as a negative term. This is not permitted according to the comments in Table A2. As a consequence, the factor  $K_f$  will have to be derived with the thermal effects of the fire compartment outer wall approximated.

An assumption that the wall material is lightweight concrete will give results on the conservative side. The factor  $K_f$  is then derived from the following expression

$$K_f = \frac{31}{50}(K_f)_D + \frac{69-31}{100}(K_f)_B = 0.62 \cdot 1.35 + 0.38 \cdot 0.85 = 1.16 \quad (h)$$

Other combinations are possible, but give higher  $K_f$ -values.

The effective values of the fire load density  $q_f$  and opening factor  $(A\sqrt{h}/A_t)_f$  will be

$$q_f = K_f \cdot q = 1.16 \cdot 127 = 147 \text{ MJ m}^{-2} \quad (\text{i})$$

$$(A\sqrt{h}/A_t)_f = K_f \cdot (A\sqrt{h}/A_t) = 1.16 \cdot 0.0569 = 0.066 \text{ m}^{1/2} \quad (\text{j})$$

### Step 3. Maximum Steel Temperature

(a) Floor assembly girders

As an initial attempt will be calculated the maximum steel temperature with the girders unprotected.

According to the table in section 3.3 the value of the resultant emissivity  $\epsilon_r$  may be chosen = 0.5. As only the lower flange of the girders is exposed to fire, the  $F_s/V_s$ -ratio is expressed by - cf. Table A4 -

$$F_s/V_s = b/bt = 1/t = 1/0.018 = 55.6 \text{ m}^{-1} \quad (\text{k})$$

For a fire compartment with enclosing structures designed according to alternative (a), Table A3 gives, with  $q_f = 166 \text{ MJ m}^{-2}$ ,  $(A\sqrt{h}/A_t)_f = 0.0745 \text{ m}^{1/2}$ ,  $\epsilon_r = 0.5$  and  $F_s/V_s = 55.6 \text{ m}^{-1}$ , the following values for the maximum steel temperature  $T_{s,\max}$

$(A\sqrt{h}/A_t)_f$	$F_s/V_s$	$T_{s,\max}$	
	50	785	
0.06	55.6	800	← interpolated value
	75	855	
	50	754	
0.08	55.6	765	← interpolated value
	75	835	

$$T_{s,\max} = 775^\circ\text{C for } (A\sqrt{h}/A_t)_f = 0.0745 \text{ m}^{1/2}$$

For the girders situated in fire compartment alternative (b) and with  $q_f = 147 \text{ MJ m}^{-2}$ ,  $(A\sqrt{h}/A_t)_f = 0.0660 \text{ m}^{1/2}$ ,  $\epsilon_r = 0.5$  and  $F_s/V_s = 55.6 \text{ m}^{-1}$  the corresponding interpolations give

$\left(\frac{A\sqrt{h}}{A_t}\right)_f$	$\frac{F_s}{V_s}$	$T_{s,max}$	
	50	730	
0.06	55.6	750	← interpolated value
	75	810	
	50	700	
0.08	55.6	720	← interpolated value
	75	795	
$T_{s,max} = 740^{\circ}\text{C}$ for $(A\sqrt{h}/A_t)_f = 0.0660 \text{ m}^{1/2}$			

(m)

Fig. 25, indicating the relation between load carrying capacity and steel temperature for a fire-exposed steel girder, shows that the computed values of  $T_{s,max}$  are too high to be acceptable. The girders will have to be protected and in a first attempt is chosen a two coat Unitherm fire retardant paint.

According to Table A6, the effective  $d_i/\lambda_i$ -value for this insulation system is  $d_i/\lambda_i = 0.065 \text{ m}^2 \text{ }^{\circ}\text{C W}^{-1}$ .

The maximum steel temperature is taken from Table A5 valid for insulated fire-exposed steel members. For the girders situated in fire compartment alternative (a) the computational scheme is as follows -  $q_f = 166 \text{ MJ m}^{-2}$ ,  $(A\sqrt{h}/A_t)_f = 0.0745 \text{ m}^{1/2}$

$$\frac{A_i}{V_s} = \frac{1}{t} = \frac{1}{0.018} = 55.6 \text{ m}^{-1} \quad (\text{Table A8}) \quad (n)$$

$$\frac{A_i \lambda_i}{V_s d_i} = \frac{55.6}{0.065} = 855 \text{ Wm}^{-30^{\circ}\text{C}^{-1}}$$

$\left(\frac{A\sqrt{h}}{A_t}\right)_f$	$\frac{A_i \lambda_i}{V_s d_i}$	$T_{s,max}$	
	600	285	
0.06	855	330	← interpolated value
	1000	375	
	600	245	
0.08	855	290	← interpolated value
	1000	330	

(o)

$$T_{s,max} = 300^{\circ}\text{C} \text{ for } (A\sqrt{h}/A_t)_f = 0.0745 \text{ m}^{1/2}$$

Corresponding calculations for fire compartment alternative (b) give  
 - with  $q_f = 147 \text{ MJ m}^{-2}$  and  $(A\sqrt{h}/A_t)_f = 0.060 \text{ m}^{1/2}$  -

$\left(\frac{A\sqrt{h}}{A_t}\right)_f$	$\frac{A_i \lambda_i}{V_s d_i}$	$T_{s,\max}$	
	600	265	
0.06	855	310	← interpolated value
	1000	350	
	600	225	
0.08	855	265	← interpolated value
	1000	305	

(p)

$$T_{s,\max} = 295^\circ\text{C for } (A\sqrt{h}/A_t)_f = 0.0660 \text{ m}^{1/2}$$

(b) Columns

The  $F_s/V_s$ -ratio of the center column is given by - cf. Table A4

$$\frac{F_s}{V_s} = \frac{2h + 4b - 2d}{\text{cross section area}} = \frac{0.38 + 0.80 - 0.013}{53.8 \cdot 10^{-4}} = 217 \text{ m}^{-1} \quad (q)$$

This  $F_s/V_s$ -value is considerably larger than the  $F_s/V_s$ -ratio for the floor assembly girders. Other circumstances being equal, the maximum steel temperature  $T_s$  will be higher than the corresponding temperature of the girders. The fact that the resultant emissivity is higher for the column, fire exposed in all sides, than for the girder - cf. section 3.3 - also works in the same direction. It follows that the centre columns must be protected.

As a first attempt, an insulation with two-coat Unitherm fire retardant paint is chosen. According to Table A6, the  $d_i/\lambda_i$ -value is  $= 0.065 \text{ m}^2 \text{ }^\circ\text{C W}^{-1}$ . The  $A_i/V_s$ -value is given by

$$\frac{A_i}{V_s} = \frac{2h + 4b - 2d}{\text{cross section area}} = 217 \text{ m}^{-1} \quad (r)$$

Hence

$$\frac{A_i \lambda_i}{V_s d_i} = \frac{217}{0.065} = 3340 \text{ W m}^{-3} \text{ }^\circ\text{C}^{-1}$$

The maximum steel temperature  $T_{s,max}$  is calculated on the basis of Table A5a for the case of columns placed inside fire compartment alternative (a) -  $q_f = 166 \text{ MJ m}^{-2}$ ,  $(A\sqrt{h}/A_t)_f = 0.0745 \text{ m}^{1/2}$

$(A\sqrt{h}/A_t)_f$	$A_i \lambda_i / V_s d_i$	$T_{s,max}$	
	3000	610	
0.06	3340	630	← interpolated value
	4000	675	
	3000	575	
0.08	3340	595	← interpolated value
	4000	640	
$T_{s,max} = 605^\circ\text{C}$ for $(A\sqrt{h}/A_t)_f = 0.0745 \text{ m}^{1/2}$			

(s)

and for the columns inside fire compartment alternative (b) with  $q_f = 147 \text{ MJ m}^{-2}$ ,  $(A\sqrt{h}/A_t)_f = 0.0660 \text{ m}^{1/2}$

$(A\sqrt{h}/A_t)_f$	$A_i \lambda_i / V_s d_i$	$T_{s,max}$	
	3000	585	
0.06	3340	605	← interpolated value
	4000	650	
	3000	540	
0.08	3340	560	← interpolated value
	4000	605	
$T_{s,max} = 590^\circ\text{C}$ for $(A\sqrt{h}/A_t)_f = 0.0660 \text{ m}^{1/2}$			

(t)

With the center columns insulated with a three coat Unitherm fire retardant paint, the effective  $d_i/\lambda_i = 0.085 \text{ m}^2 \text{ }^\circ\text{C W}^{-1}$  (cf. Table A6), and an analogous calculation gives the maximum steel temperatures

$$T_{s,max} = 545^\circ\text{C} \quad (u)$$

for fire compartment alternative (a)

$$T_{s,max} = 530^\circ\text{C} \quad (v)$$

for fire compartment alternative (b).

#### Step 4. Calculation of Critical Loads

##### (a) Floor assembly girders

The calculations in the last section demonstrated that the maximum steel temperature of the floor assembly beams, insulated with a two coat Unitherm fire retardant paint, was nearly identical for the two fire compartment alternatives. The maximum value is - cf. Eqs. (o) and (p)

$$T_{s,max} = 300^{\circ}\text{C}$$

The corresponding smallest value of the load carrying capacity or the critical load is obtained from Fig. 25. As the maximum temperature does not exceed  $450^{\circ}\text{C}$ , the influence of creep deformation and variation in heating up rate can be neglected, implying that Fig. 26 lacks relevance in this instance.

For existing loading and supporting conditions, curve No. 2 in Fig. 25 is applicable, and the value of the critical load  $q_{cr}$  is given by

$$\beta = 0.95$$

$$q_{cr} = \beta \frac{8\sigma_s W}{L^2} = 0.95 \frac{8 \cdot 260 \cdot 10^3 \cdot 1.38 \cdot 10^{-3}}{7^2} = 55.7 \text{ kN m}^{-1} \quad (x)$$

which exceeds the design load  $= 37 \text{ kN m}^{-1}$  - see step 1. The conclusion is, that with the chosen fire protection, the floor assembly girders will be able to fulfil their load carrying function throughout the complete fire exposure.

##### (b) Columns

The columns are assumed to be unbraced between the floor assembly levels. Buckling in the weak axis direction will be decisive. It is further assumed that the support condition of the columns are such that the effective buckling length  $L$  is equal to the centrum distance between the floor assemblies, 2.8 m.

The slenderness ratio  $\lambda$  of the center columns will be, with  $i_{min}$  denoting the least radius of gyration of the cross-sectional area



$$\lambda = \frac{L}{i_{\min}} = \frac{2.8}{0.0498} = 56 \quad (y)$$

With known values for the slenderness ratio  $\lambda$  and maximum steel temperature  $T_{s,\max}$  the allowable buckling stress  $\sigma_{cr}$  is obtained from Fig. 27. (The steel quality of the columns corresponds to a nominal yield strength at room temperature  $\sigma_s = 260$  MPa).

For the center columns inside fire compartment alternative (a) and insulated with a two coat Unitherm fire retardant paint, the following values are obtained

$$T_{s,\max} = 605^{\circ}\text{C}, \text{ Eq. (s)}$$

$$\sigma_{cr} = 62 \text{ MPa}$$

$$N_{cr} = \sigma_{cr} A = 62 \cdot 53.8 \cdot 10^{-4} = 0.335 \text{ MN} = 335 \text{ kN} \quad (z)$$

The minimum value of the buckling load  $N_{cr}$  in this case falls below the calculated design load  $N = 484$  kN. The insulation with a two-coat Unitherm fire retardant paint is insufficient for fire compartment alternative (a). An increase in the Unitherm-insulation to a three-coat painting gives

$$T_{s,\max} = 545^{\circ}\text{C}, \text{ Eq. (u)}$$

$$\sigma_{cr} = 87 \text{ MPa}$$

$$N_{cr} = 87 \cdot 53.8 \cdot 10^{-4} = 0.470 \text{ MN} = 470 \text{ kN} \quad (\text{aa})$$

and the fire protection is still insufficient. The difference from the required capacity of 484 kN is quite small however. It is surmised that an increase in the insulating capacity, i.e. the  $d_i/\lambda_i$ -value, from  $0.085 \text{ m}^2 \text{ }^{\circ}\text{C W}^{-1}$ , valid for the three coat Unitherm treatment, to  $0.09 \text{ m}^2 \text{ }^{\circ}\text{C W}^{-1}$  should give adequate protection. With sprayed mineral wool as fire insulation material, this insulating capacity is obtained with a layer thickness  $d_i$  of 10 mm, see Table A6, which gives the variation of thermal conductivity  $\lambda_i$  with temperature for a number of insulating materials. Assuming that the average insulation temperature approximately is equal to maximum steel temperature  $T_{s,\max} \approx 525^{\circ}\text{C}$ , Table A6 gives

$$\lambda_i = 0.10 \text{ W m}^{-1} \text{ }^{\circ}\text{C}^{-1}$$

$$\frac{d_i}{\lambda_i} = \frac{0.01}{0.10} = 0.1 \text{ m}^2 \text{ }^{\circ}\text{C W}^{-1}$$

Consequently, adequate fire protection for the columns is offered by the application of 10 mm sprayed mineral wool.

For the centre columns inside fire compartment alternative (b) and protected with a three-coat Unitherm fire retardant paint the calculations show

$$T_{s,\max} = 530^{\circ}\text{C}, \text{ Eq. (v)}$$

$$\sigma_{cr} = 93 \text{ MPa}$$

$$N_{cr} = 93 \cdot 53.8 \cdot 10^{-4} = 0.500 \text{ MN} = 500 \text{ kN} \quad (\text{ab})$$

i.e. a minimum buckling load exceeding the required design load  $N = 484 \text{ kN}$ . A protection with a three coat-Unitherm fire retardant paint is obviously sufficient under these conditions.

It is assumed, when calculating the buckling loads, that the columns are free to longitudinally expand during the thermal exposure from the fire. For design situation where this assumption is not valid, the calculations must be based on design curves, specifically taking into account the effect of a partially restrained thermal expansion. Reference is made to [4].

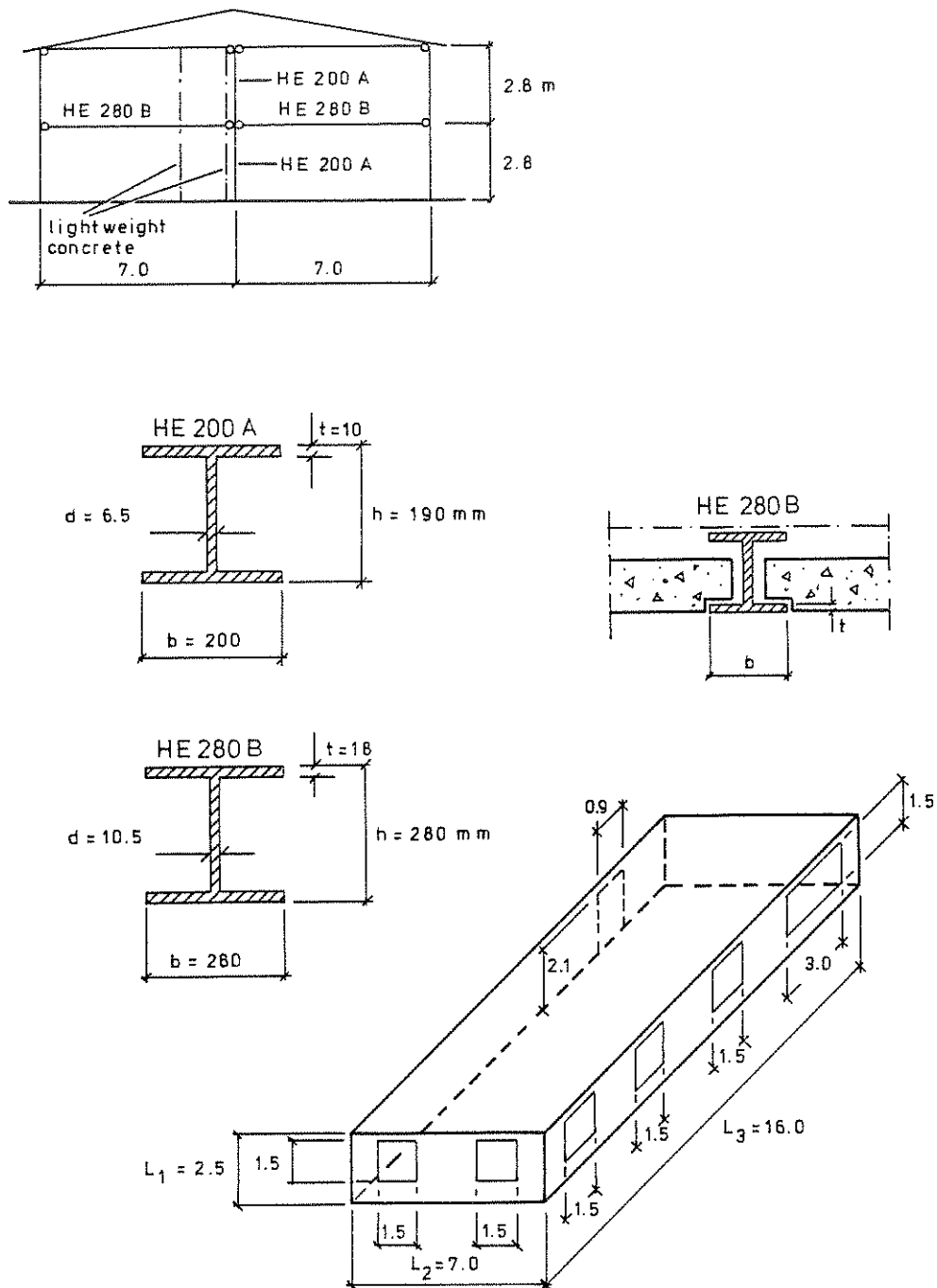


Figure 30.

## References

- [1] MAGNUSSON, S.E. and PETTERSSON, O.: Functional Approaches - An Outline. Final Report, CIB W14 Symposium "Fire Safety in Buildings: Needs and Criteria", held in Amsterdam 1977-06-02/03, p. 120-145.
- [2] NATIONAL SWEDISH BOARD OF PHYSICAL PLANNING AND BUILDING: Brandteknisk dimensionering (Fire Engineering Design). Comments on SBN (Swedish Building Code), No. 1976:1.
- [3] PETTERSSON, O.: Principles of Fire Engineering Design and Fire Safety of Tall Buildings. ASCE-IABSE International Conference on Planning and Design of Tall Buildings, Lehigh University, Bethlehem, Pa., August 21-26, 1972, Summary Report of Technical Committee 8, Conference Preprints, Vol. DS. - Bulletin 31, Division of Structural Mechanics and Concrete Construction, Lund Institute of Technology, Lund, 1973.
- [4] PETTERSSON, O., MAGNUSSON, S.E. and THOR, J.: Fire Engineering Design of Steel Structures. Swedish Institute of Steel Construction, Publication No. 50, Stockholm 1976 (Swedish edition 1974).
- [5] PETTERSSON, O.: Calcul Théoretique des Structures Exposées au Feu. Sécurité de la Construction Face à L'Incendie, Séminaire tenu à Saint-Rémy-lès Chevreuse (France) du 18 au 20 Novembre 1975, Editions Eyrolles, Paris, 1977, pp. 175-224. - Theoretical Design of Fire Exposed Structures. Bulletin 51, Division of Structural Mechanics and Concrete Construction, Lund Institute of Technology, Lund, 1976.
- [6] PETTERSSON, O. and ØDEEN, K.: Brandteknisk dimensionering av byggnadskonstruktioner - principer, underlag, exempel (Fire Engineering Design of Building Structures - Principles, Design Basis, Examples). Liber Förlag, Stockholm, 1978.
- [7] NATIONAL SWEDISH BOARD OF PHYSICAL PLANNING AND BUILDING, Safety Group: Allmänna bestämmelser för bärande konstruktioner, AK 77, del 1. Säkerhetsbestämmelser (General Regulations for Load-Bearing Structures, AK 77, Part 1, Safety Regulations). Draft Proposal, Stockholm, 1976-11-24.

- [8] ANG, H.S. and CORNELL, C.A.: Reliability Basis of Structural Safety and Design. Journal of the Structural Division, ASCE, Vol. 100, No. ST9, Proc. Paper 10777, September 1974, pp. 1755-1769.
- [9] ELLINGWOOD, R. and ANG, H.S.: Risk-Based Evaluation of Design Criteria. Journal of the Structural Division, ASCE, Vol. 100, No. ST9, Proc. Paper 10778, September 1974, pp. 1771-1788.
- [10] MAGNUSSON, S.E.: Probabilistic Analysis of Fire Exposed Steel Structures. Bulletin 27, Division of Structural Mechanics and Concrete Construction, Lund Institute of Technology, Lund, 1974.
- [11] LAW, M.: Design Guide for Fire Safety of Bare Exterior Structural Steel. 1. Theory and Validation. 2. State of the Art. Ove Arup & Partners. London, January 1977.
- [12] BECHTOLD, R.: Zur thermischen Beanspruchung von Aussenstützen im Brandfall. Heft 37, Institut für Baustoffkunde und Stahlbetonbau, Technische Universität, Braunschweig, September 1977.
- [13] KAWAGOE, K. and SEKINE, T.: Estimation of Fire Temperature-Time Curve in Rooms. Occasional Report No. 11, Building Research Institute, Tokyo, 1963. - KAWAGOE, K.: Estimation of Fire Temperature-Time Curve in Rooms. Research Paper No. 29, Building Research Institute, Tokyo, 1967.
- [14] ØDEEN, K.: Theoretical Study of Fire Characteristics in Enclosed Spaces. Bulletin 19, Division of Building Construction, Royal Institute of Technology, Stockholm, 1963.
- [15] MAGNUSSON, S.E. and THELANDERSSON, S.: Temperature-Time Curves for the Complete Process of Fire Development. A Theoretical Study of Wood Fuel Fires in Enclosed Spaces. Acta Polytechnica Scandinavica, Ci 65, Stockholm, 1970.
- [16] MAGNUSSON, S.E. and THELANDERSSON, S.: A Discussion of Compartment Fires. Fire Technology, Vol. 10, No. 3, August 1974.

- [17] HARMATHY, T.Z.: A New Look at Compartment Fires. Part I, Fire Technology, Vol. 8, No. 3, August 1972, and Part II, Fire Technology, Vol. 8, No. 4, November 1972.
- [18] BABRAUSKAS, V. and WILLIAMSON, R.B.: Post-Flashover Compartment Fires. University of California, Berkeley, Fire Research Group, Report No. UCB FRG 75-1, December 1975. - Post-Flashover Compartment Fires: Basis of a Theoretical Model. Fire and Materials, Vol. 2, No. 2, April 1978.
- [19] THOMAS, P.H.: Some Problem Aspects of Fully Developed Room Fires. Symposium on "Fire Standards and Safety", Washington, 5-6 April 1976.
- [20] NILSSON, L.: Brandbelastning i bostadslägenheter (Fire Loads in Flats). National Swedish Institute for Building Research, Report No. 34, Stockholm, 1970.
- [21] THOMAS, P.H. - HINKLEY, P.L. - THEOBALD, C.R. - SIMMS, D.L.: Investigations into the Flow of Hot Gases in Roof Venting. Fire Research Technical Paper No. 7, Fire Research Station, London, 1963.
- [22] THOR, J.: Strålningspåverkan på oisolerade eller undertaksisolerade stålkonstruktioner vid brand (Radiation Effects of Fire on Steel Structures either without Insulation or Insulated by a Ceiling). Division of Structural Mechanics and Concrete Construction, Lund Institute of Technology, Bulletin No. 29, Lund, Sweden, 1972.
- [23] ØDEEN, K. and ANAS, B.: Brandskyddande undertak för stålkonstruktioner (Fire Protection for Steel Structures in the Form of a Suspended Ceiling). Byggmästaren No. 12, Stockholm, 1969.
- [24] WICKSTRÖM, U.: A Numerical Procedure for Calculating Temperature in Hollow Structures Exposed to Fire. Fire Research Group, University of California, Report No. UCB FRG 77-9, Berkeley, August 1977.

- [25] MAGNUSSON, S.E. and PETTERSSON, O.: Brandteknisk dimensionering av isolerad stålkonstruktion i bärande eller avskiljande funktion (Fire Engineering Design of Insulated Load-Bearing or Separating Steel Structures). Väg- och vattenbyggaren No. 4, Stockholm, 1969.
- [26] HARMATHY, T.Z.: A Treatise on Theoretical Fire Endurance Rating. Research Paper No. 153, Division of Building Research, National Research Council, Canada, Ottawa, 1962.
- [27] THOR, J.: Deformations and Critical Loads of Steel Beams Under Fire Exposure Conditions. National Swedish Building Research, Document D16:1973, Stockholm.
- [28] ROBERTSON, A.F. and RYAN, I.V.: Proposed Criteria for Defining Load Failure of Beams, Floors and Roof Constructions during Fire Tests. Journal of Research, National Bureau of Standards, Vol. 63 C, Washington, 1959.
- [29] KRUPPA, J.: Résistance au Feu des Structures Métalliques en Température Non Homogène. Thèse, Présentée devant l'Institut National des Sciences Appliquées de Rennes pour l'obtention du grade de Docteur-Ingenieur en Genie Civil, 27 Juin 1977.

## APPENDIX

Table A1. Fire load characteristics according to recent Swedish investigations - fire load density  $q$  defined according to Eq (3) with  $\mu_v=1$

Type of fire compartment	Average $\text{Mcal}\cdot\text{m}^{-2}$ $\{\text{MJ}\cdot\text{m}^{-2}\}$	Standard deviation $\text{Mcal}\cdot\text{m}^{-2}$ $\{\text{MJ}\cdot\text{m}^{-2}\}$	Design value $\text{Mcal}\cdot\text{m}^{-2}$ $\{\text{MJ}\cdot\text{m}^{-2}\}$
1 Dwellings <sup>1)</sup>			
1a Two rooms and a kitchen	35.8 {150}	5.9 {24.7}	40.0 {168}
1b Three rooms and a kitchen	33.1 {139}	4.8 {20.1}	35.5 {149}
2 Offices <sup>2)</sup>			
2a Technical offices	29.7 {124}	7.5 {31.4}	34.5 {145}
2b Administrative offices	24.3 {102}	7.7 {32.2}	31.5 {132}
2c All offices, investigated	27.3 {114}	9.4 {39.4}	33.0 {138}
3 Schools <sup>2)</sup>			
3a Schools - junior level	20.1 {84.2}	3.4 {14.2}	23.5 {98.4}
3b Schools - middle level	23.1 {96.7}	4.9 {20.5}	28.0 {117}
3c Schools - senior level	14.6 {61.1}	4.4 {18.4}	17.0 {71.2}
3d All schools, investigated	19.2 {80.4}	5.6 {23.4}	23.0 {96.3}
4 Hospitals	27.6 {116}	8.6 {36.0}	35.0 {147}
5 Hotels <sup>2)</sup>	16.0 {67.0}	4.6 {19.3}	19.5 {81.6}

1) Floor covering excluded

2) Only moveable fire load components included



Table A2. Coefficient  $K_f$  for transforming a real fire load density  $q$  and a real opening factor of a fire compartment  $A\sqrt{h}/A_t$  to an effective fire load density  $q_f$  and an effective opening factor  $(A\sqrt{h}/A_t)_f$  corresponding to a fire compartment, type A

$$q_f = K_f q$$

$$(A\sqrt{h}/A_t)_f = K_f A\sqrt{h}/A_t$$

Type of fire compartment	Opening factor $A\sqrt{h}/A_t \quad m^{1/2}$					
	0.02	0.04	0.06	0.08	0.10	0.12
Type A	1	1	1	1	1	1
Type B	0.85	0.85	0.85	0.85	0.85	0.85
Type C	3.00	3.00	3.00	3.00	3.00	2.50
Type D	1.35	1.35	1.35	1.50	1.55	1.65
Type E	1.65	1.50	1.35	1.50	1.75	2.00
Type F <sup>1)</sup>	1.00-	1.00-	0.80-	0.70-	0.70-	0.70-
	0.50	0.50	0.50	0.50	0.50	0.50
Type G	1.50	1.45	1.35	1.25	1.15	1.05
Type H	3.00	3.00	3.00	3.00	3.00	2.50

<sup>1)</sup> The lowest value of  $K_f$  applies to a fire load density  $q > 500 \text{ MJ}\cdot\text{m}^{-2}$ , the highest value to a fire load density  $q \leq 60 \text{ MJ}\cdot\text{m}^{-2}$ . For intermediate fire load densities, linear interpolation gives sufficient accuracy.

The different types of fire compartment are defined as follows

Fire compartment, type B: Bounding structures of concrete.

Fire compartment, type C: Bounding structures of lightweight concrete (density  $\rho = 500 \text{ kg}\cdot\text{m}^{-3}$ ).

Fire compartment, type D: 50% of the bounding structures of concrete, and of 50% lightweight concrete (density  $\rho = 500 \text{ kg}\cdot\text{m}^{-3}$ ).

Fire compartment, type E: Bounding structures with the following percentage of bounding surface area:

50% lightweight concrete (density  $\rho = 500 \text{ kg}\cdot\text{m}^{-3}$ ),  
33% concrete,

17% of from the interior to the exterior: plasterboard panel (density  $\rho = 790 \text{ kg}\cdot\text{m}^{-3}$ ), 13 mm in thickness - diabase wool (density  $\rho = 50 \text{ kg}\cdot\text{m}^{-3}$ ), 10 cm in thickness - brickwork (density  $\rho = 1800 \text{ kg}\cdot\text{m}^{-3}$ ), 20 cm in thickness.

Fire compartment, type F: 80% of the bounding structures of sheet steel, and 20% of concrete. The compartment corresponds to a storage space with a sheet steel roof, sheet steel walls, and a concrete floor.

Fire compartment, type G: Bounding structures with the following percentage of bounding surface area:

20% concrete,

80% of from the interior to the exterior: double plasterboard panel (density  $\rho = 790 \text{ kg}\cdot\text{m}^{-3}$ ), 2x13 mm in thickness - air space, 10 cm in thickness - double plasterboard panel (density  $\rho = 790 \text{ kg}\cdot\text{m}^{-3}$ ), 2x13 mm in thickness.

Fire compartment, type H: Bounding structures of sheet steel on both sides of diabase wool (density  $\rho = 50 \text{ kg}\cdot\text{m}^{-3}$ ), 10 cm in thickness.

For fire compartments, not directly represented in the table, the coefficient  $K_f$  can either be determined by a linear interpolation between applicable types of fire compartment in the table or be chosen in such a way as to give results on the safe side. For fire compartments with surrounding structures of both concrete and lightweight concrete, then different values can be obtained of the coefficient  $K_f$ , depending on the choice between the fire compartment types B, C, and D at the interpolation. This is due to the fact that the relationships, determining  $K_f$ , are non-linear. However, the  $K_f$ -values of the table are such that a linear interpolation always gives results on the safe side, irrespective of the alternative of interpolation chosen. In order to avoid an unnecessarily large overestimation of  $K_f$ , that alternative of interpolation is recommended which gives the lowest value of  $K_f$ . At the determination of  $K_f$ , it is not allowed to combine types of fire compartments in such a way, that any of them gives a negative contribution to  $K_f$ .

Table A3. Maximum steel temperature  $T_{s,max}$  ( $^{\circ}\text{C}$ ) for unisolated steel structure as a function of effective fire load density  $q$  ( $\text{Mcal}\cdot\text{m}^{-2}$ )  $\{\text{MJ}\cdot\text{m}^{-2}\}$ , effective opening factor  $A\sqrt{h}/A_t$  ( $\text{m}^{1/2}$ ),  $F_s/V_s$  ratio ( $\text{m}^{-1}$ ), and resultant emissivity  $\epsilon_r$  [4]

q	$\frac{A\sqrt{h}}{A_t}$	$\frac{F_s}{V_s}$	$T_{s,max}$				q	$\frac{A\sqrt{h}}{A_t}$	$\frac{F_s}{V_s}$	$T_{s,max}$				q	$\frac{A\sqrt{h}}{A_t}$	$\frac{F_s}{V_s}$	$T_{s,max}$						
			$\epsilon_r$	$\epsilon_r$	$\epsilon_r$	$\epsilon_r$				$\epsilon_r$	$\epsilon_r$	$\epsilon_r$	$\epsilon_r$										
																	0,3	0,5	0,7	0,3	0,5	0,7	
10 {42}	0,01	50	325	345	370	15 {63}	0,01	50	400	420	440	20 {84}	0,01	25	390	425	445	25 {105}	0,01	25	455	490	500
		75	365	385	405			75	435	445	460			50	465	480	490			50	510	525	530
		100	395	410	425			100	450	460	470			75	485	500	500			75	525	530	535
		125	410	425	435			125	460	470	475			100	495	505	505			100	530	535	535
		150	425	435	440			150	470	475	480			125	500	505	510			125	530	535	540
		200	435	445	445			200	475	480	480			150	505	510	510			150	535	540	540
	0,02	400	450	450	450		400	480	485	485	200		505	510	515	300	535		540	540			
		50	335	380	410		50	425	480	515	400		510	515	515	50	555		600	625			
		75	410	445	475		75	500	540	565	50		500	550	575	75	610		640	650			
		100	445	490	520		100	640	575	595	75		560	600	620	100	640		650	655			
		125	480	520	545		125	565	600	610	100		595	620	630	125	650		655	660			
		150	500	540	555		150	585	605	615	125		615	630	640	150	670		685	700			
	0,04	200	540	560	575		200	605	620	625	150		625	640	645	200	670		685	700			
		400	575	585	585		400	625	630	630	200		635	645	650	200	670		685	700			
		50	285	320	365		50	400	455	510	400		650	650	650	25	355		420	510			
		75	350	400	450		75	490	550	600	50		485	565	625	50	525		580	700			
		100	405	460	510		100	550	610	655	75		555	650	700	75	640		690	780			
		125	430	515	535		125	600	655	690	100		650	700	740	100	660		775	-			
	0,06	150	485	555	595		150	635	680	710	125		650	700	735	125	650		715	-			
		200	530	605	645		200	650	700	755	150		670	715	790	150	670		715	-			
		300	625	660	690		300	625	725	785	200		680	715	790	200	680		715	-			
		50	235	275	330		50	340	400	475	25		255	340	415	25	240		260	385			
		75	305	370	425		75	425	500	570	50		310	375	500	50	400		460	590			
		100	365	410	485		100	500	550	630	75		435	480	610	75	500		580	700			
	0,08	125	415	455	545		125	550	600	680	100		565	670	735	100	560		565	560			
		150	450	485	580		150	590	630	720	125		615	630	735	125	560		565	565			
		200	520	555	660		200	650	700	755	150		650	685	-	150	560		565	565			
		300	615	650	735		300	625	725	785	200		680	715	790	200	565		565	570			
		50	200	255	300		50	260	290	400	25		230	285	365	25	500		570	570			
		75	270	330	400		75	340	380	500	50		490	505	515	50	600		640	660			
	0,12	100	330	400	460		100	390	400	600	75		510	515	520	75	650		670	670			
		125	360	450	510		125	450	540	675	100		520	520	520	100	660		675	675			
		150	410	510	550		150	500	600	750	125		550	620	775	125	630		705	750			
		200	480	590	660		200	575	680	-	150		600	685	-	150	630		705	750			
		300	600	700	760		300	625	725	785	200		680	715	790	200	630		705	750			
		50	170	200	260		50	260	290	400	25		430	460	480	25	410		500	590			
0,1	75	220	260	350	75	340	380	500	50	490	505	515	50	595	630	700							
	100	240	310	400	100	390	400	600	75	510	515	520	75	705	775	-							
	125	260	380	540	125	450	540	675	100	520	520	520	100	565	665	745							
	150	310	430	620	150	500	600	750	125	550	620	775	125	565	665	745							
	200	380	500	700	200	575	680	-	150	600	685	-	150	565	665	745							
	300	450	620	800	300	625	725	785	200	680	715	790	200	565	665	745							
12,5 {52,5}	0,01	50	365	385	405	17,5 {73,5}	0,01	50	460	515	550	22,5 {94,5}	0,01	100	615	635	650	45 {190}	0,01	100	660	675	675
		75	410	425	435			75	430	445	450			100	615	635	650			100	660	675	675
		100	430	445	450			100	460	475	480			125	630	645	650			125	630	645	650
		125	440	450	460			125	480	485	490			150	645	650	655			150	645	650	655
		150	450	455	460			150	485	490	495			200	650	660	665			200	650	660	665
		200	455	460	465			200	485	495	500			300	655	660	660			300	655	660	660
	0,02	400	465	470	470		400	490	500	500	400		660	660	660	400	660		660	660			
		50	350	435	470		50	530	570	595	50		530	575	605	50	565		665	745			
		75	455	500	535		75	565	600	615	75		590	620	635	75	600		630	650			
		100	500	540	560		100	610	620	635	100		615	635	650	100	615		635	650			
		125	525	555	575		125	635	645	645	125		630	645	650	125	630		645	650			
		150	550	570	580		150	650	660	665	150		645	650	655	150	645		650	655			
	0,04	200	570	590	600		200	660	660	670	200		650	660	665	200	650		660	665			
		400	600	605	605		400	650	700	740	300		655	660	660	300	655		660	660			
		50	340	400	450		50	255	300	370	50		430	540	605	50	430		540	605			
		75	415	455	540		75	390	455	550	75		465	540	630	75	465		540	630			
		100	485	550	600		100	565	620	710	100		610	615	750	100	610		615	750			
		125	535	600	640		125	620	670	750	125		625	675	800	125	625		675	800			
	0,06	150	570	625	665		150	650	700	750	150		650	740	-	150	650		740	-			
		200	630	665	700		200	650	700	750	200		650	740	-	200	650		740	-			
		50	290	335	400		50	345	435	490	50		435	550	605	50	435		550	605			
		75	365	425	495		75	440	530	600	75		460	550	605	75	460		550	605			
		100	425	480	560		100	500	605	670	100		500	605	670	100	500		605	670			
		125	480	535	610		125	565	650	740	125		565	650	740	125	565		650	740			
	0,08	150	520	560	650		150	515	705	765	150		515	705	765	150	515		705	765			
		200	580	625	705		200	575	660	740	200		575	660	740	200	575		660	740			
		300	670	740	770		300	650	740	770	300		650	740	770	300	650		740	770			
		50	250	315	360		50	275	330	450	25		160	200	275	25	160		200	275			
		75	325	400	455		75	350	430	550	50		225	275	325	50	225		275	325			
		100	385	475	535		100	425	505	650	100		425	505	650	100	425		505	650			
	0,12	125	435	530	600		125	475	575	725	125		475	575	725	125	475		575	725			
		150	485	585	650		150	525	645	775	150		525	645	775	150	525		645	775			
		200	530	660	730		200	600	725	-	200		600	725	-	200	600		725	-			
		300	655	770	-		300	600	725	-	300		600	725	-	300	600		725	-			
		50	200	250	330		50	240	320	410	25		180	240	310	25	180		240	310			
		75	240	320	410		75	280	360	450	50		220	300	390	50	220		300	390			

Table A4.  $F_s/V_s$  for different types of fire exposed, uninsulated steel structures

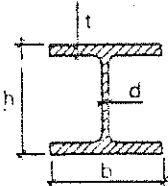
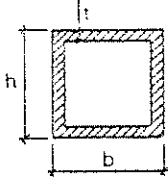
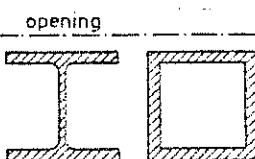
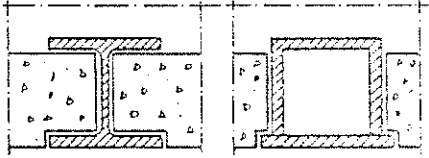
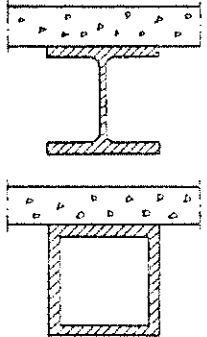
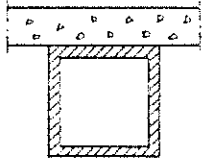
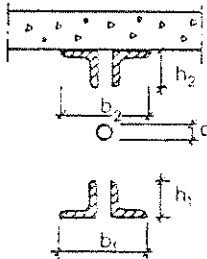
Column within a fire compartment		$\frac{F_s}{V_s} = \frac{2h + 4b - 2d}{\text{cross section area}}$
		$\frac{F_s}{V_s} = \frac{2h + 2b}{\text{cross section area}}$
Column, immediately outside a window opening		$\frac{F_s}{V_s} = \frac{2h + b}{\text{cross section area}}$
Floor structure, composed of steel beams with a concrete slab, supported on the lower flange of the beams		$\frac{F_s}{V_s} = \frac{b}{bt} = \frac{1}{t}$
Beams with a floor slab, supported on the upper flange of the beams		$\frac{F_s}{V_s} = \frac{2h + 3b - 2d}{\text{cross section area}}$
		$\frac{F_s}{V_s} = \frac{2h + b}{\text{cross section area}}$
Floor slab beams of truss type ( $F_s/V_s$ is determined for each part of the truss)		$\frac{F_s}{V_s} \text{ (lower flange)} = \frac{2b_1 + 2h_1}{\text{cross section area of lower flange}}$ $\frac{F_s}{V_s} \text{ (upper flange)} = \frac{b_2 + 2h_2}{\text{cross section area of upper flange}}$ $\frac{F_s}{V_s} \text{ (diagonal)} = \frac{4}{d}$

Table A5. Maximum steel temperature  $T_{s,max}$  ( $^{\circ}\text{C}$ ) for insulated steel structures as a function of effective fire load density  $q_f$  ( $\text{MJ m}^{-2}$ ), effective opening factor  $(A\sqrt{h}/A_t)_f$  ( $\text{m}^{1/2}$ ) and the design parameter  $A_i \lambda_i / (V_s d_i)$  ( $\text{W m}^{-3} \text{h}^{-1} \text{ } ^{\circ}\text{C}^{-1}$ ) [6]

$$(A\sqrt{h}/A_t)_f = 0.01 \text{ m}^{1/2}$$

$q_f$	$A_i \lambda_i / (V_s d_i)$													
	50	100	200	400	600	1000	1500	2000	3000	4000	6000	8000	10000	
13	30	40	50	70	90	115	140	160	190	210	235	260	280	
19	35	45	65	95	115	150	180	205	245	265	295	320	340	
25	40	55	80	115	145	180	220	245	285	305	335	360	375	
50	60	90	135	190	225	280	325	350	390	410	430	440	450	
75	80	125	180	250	295	355	400	430	455	470	480	490	490	
100	100	155	225	310	365	430	470	490	510	520	530	530	535	
125	115	185	270	370	425	485	520	535	550	555	560	560	565	

$$(A\sqrt{h}/A_t)_f = 0.02 \text{ m}^{1/2}$$

$Q_f$	$A_i \lambda_i / (V_s d_i)$													
	50	100	200	400	600	1000	1500	2000	3000	4000	6000	8000	10000	
13	25	30	40	60	70	90	110	130	165	185	215	245	270	
25	35	45	65	90	120	155	190	220	270	300	335	375	405	
38	40	55	85	125	160	205	250	290	345	380	420	460	485	
50	45	70	105	155	195	250	305	345	400	435	480	515	535	
100	75	115	175	250	305	385	450	490	550	580	610	630	635	
150	100	155	235	330	405	490	555	595	640	660	680	690	695	
200	125	195	290	415	495	585	645	680	710	725	735	740	745	
250	145	235	355	490	570	655	705	730	755	765	775	780	780	

$$(A\sqrt{h}/A_t)_f = 0.04 \text{ m}^{1/2}$$

$q_f$	$A_i \lambda_i / (V_s d_i)$													
	50	100	200	400	600	1000	1500	2000	3000	4000	6000	8000	10000	
25	25	35	50	70	85	115	140	170	210	245	290	330	365	
50	35	50	75	115	150	200	245	290	350	395	450	505	540	
75	45	65	100	155	200	260	325	380	450	500	565	615	650	
100	50	80	125	190	245	320	395	450	525	575	640	685	715	
200	85	135	210	310	385	490	575	635	710	755	800	825	835	
300	115	180	275	410	500	615	700	755	815	845	875	890	895	
400	140	225	345	505	605	720	800	845	890					
500	170	270	415	585	685	790	860	895						

$$(A\sqrt{h}/A_t)_f = 0.06 \text{ m}^{1/2}$$

$q_f$	$A_i \lambda_i / (V_s d_i)$												
	50	100	200	400	600	1000	1500	2000	3000	4000	6000	8000	10000
38	30	35	50	75	95	125	160	190	240	280	330	380	420
75	35	50	80	125	165	220	275	325	395	450	515	580	625
113	45	70	110	170	220	290	365	425	510	570	645	705	740
150	55	85	135	210	270	355	440	500	590	655	730	780	810
300	90	140	225	335	420	540	635	705	790	840	890		
450	120	190	295	440	540	670	765	825	895				
600	150	240	370	545	650	780	865						
750	175	285	445	625	730	850							

$$(A\sqrt{h}/A_t)_f = 0.08 \text{ m}^{1/2}$$

$q_f$	$A_i \lambda_i / (V_s d_i)$												
	50	100	200	400	600	1000	1500	2000	3000	4000	6000	8000	10000
50	30	35	55	80	100	135	170	205	260	300	355	410	455
100	35	55	85	130	170	235	295	350	425	485	560	625	675
150	45	70	115	180	230	310	390	455	545	610	695	755	800
200	55	85	140	220	280	380	470	535	635	700	780	835	870
400	90	145	230	350	440	565	670	745	835	890			
600	120	195	305	460	565	705	805	865					
800	150	245	380	565	675	810							
1000	180	295	455	650	760								

$$(A\sqrt{h}/A_t)_f = 0.12 \text{ m}^{1/2}$$

$q_f$	$A_i \lambda_i / (V_s d_i)$												
	50	100	200	400	600	1000	1500	2000	3000	4000	6000	8000	10000
75	30	40	55	85	105	140	180	220	280	330	390	450	495
150	40	55	90	140	185	250	320	375	465	525	615	685	740
225	45	75	120	190	245	330	420	490	590	660	755	820	870
300	55	90	145	230	300	405	500	575	680	755	840		
600	95	150	240	365	465	600	710	790	890				
900	125	200	315	480	595	735	845						
1200	155	250	395	585	705	845							
1500	185	305	470	670	785								

$$(A\sqrt{h}/A_t)_f = 0.30 \text{ m}^{1/2}$$

$q_f$	$A_i \lambda_i / (V_s d_i)$												
	50	100	200	400	600	1000	1500	2000	3000	4000	6000	8000	10000
188	30	40	60	90	115	155	205	245	320	375	445	515	570
375	40	60	95	150	200	275	355	420	515	590	695	770	835
563	50	75	125	200	265	365	460	540	655	735	845		
750	60	95	155	250	320	440	550	630	750	830			
1500	95	155	250	390	495	640	765	850					
2250	130	210	330	510	630	785	900						
3000	160	260	415	615	740	890							
3750	190	315	490	700	820								

Table A6. Thermal conductivity  $\lambda_i$  ( $\text{kcal}\cdot\text{m}^{-1}\cdot^\circ\text{C}^{-1}\cdot\text{h}^{-1}$ )  $\{\text{Wm}^{-1}\cdot^\circ\text{C}^{-1}\}$  of some insulation materials as a function of the insulation temperature [4]

	Temperature $^\circ\text{C}$										
	0	100	200	300	400	500	600	700	800	900	1000
Sprayed mineral wool Calco Blaze-Shield Type DC/F	0,045 {0,053}	0,047 {0,055}	0,050 {0,058}	0,058 {0,066}	0,066 {0,077}	0,077 {0,090}	0,095 {0,110}	0,120 {0,140}	0,145 {0,170}	0,170 {0,198}	0,210 {0,245}
Sprayed mineral wool Type Pyroguard 101	0,044 {0,051}	0,055 {0,064}	0,059 {0,069}	0,066 {0,077}	0,071 {0,083}	0,079 {0,092}	0,089 {0,104}	0,103 {0,120}	0,123 {0,144}	0,150 {0,175}	0,190 {0,220}
Fire retardant plaster Type Jimoterm	0,203 {0,236}	0,145 {0,169}	0,144 {0,168}	0,143 {0,167}	0,141 {0,165}	0,138 {0,161}	0,138 {0,161}	0,156 {0,182}	0,182 {0,212}	0,186 {0,217}	—
Fire retardant plaster Type Pyrodur	0,085 {0,099}	0,090 {0,105}	0,095 {0,110}	0,100 {0,116}	0,105 {0,122}	0,110 {0,128}	0,115 {0,134}	0,115 {0,134}	0,120 {0,140}	0,125 {0,146}	0,130 {0,152}
Slabs of vermiculite based material Type Vermit fire insulation slab	0,077 {0,090}	0,085 {0,099}	0,092 {0,108}	0,100 {0,116}	0,112 {0,130}	0,117 {0,137}	0,125 {0,146}	0,133 {0,155}	0,145 {0,169}	0,157 {0,183}	0,171 {0,199}
Mineral wool slabs with a density of $\gamma \approx 150 \text{ kg/m}^3$ Type Minwool slab 3060 or Rockwool slab 337	0,030 {0,035}	0,044 {0,051}	0,058 {0,068}	0,081 {0,094}	0,109 {0,127}	0,149 {0,173}	0,187 {0,218}	0,235 {0,275}	0,280 {0,325}	0,365 {0,425}	0,470 {0,550}
Gypsum plaster slabs Type Gyproc	0,180 {0,210}	0,180 {0,210}	0,120 {0,140}	0,135 {0,157}	0,155 {0,181}	0,170 {0,198}	0,190 {0,220}	0,205 {0,240}	0,225 {0,260}	0,250 {0,290}	0,275 {0,320}
Prefabricated gypsum plaster sections Type GPG	0,250 {0,290}	0,130 {0,152}	0,124 {0,145}	0,133 {0,155}	0,135 {0,157}	0,130 {0,152}	—	—	—	—	—
Prefabricated gypsum plaster sections Type Perlitgips	0,180 {0,210}	0,105 {0,122}	0,084 {0,098}	0,106 {0,123}	0,115 {0,134}	0,122 {0,142}	—	—	—	—	—

#### Fire retardant paints

Most fire retardant paints change in thickness on exposure to fire. Information relating only to the variation of the thermal conductivity with temperature does not therefore provide a sufficient basis for design. The insulation capacity of the paint, expressed in terms of a fictive  $d_i/\lambda_i$  value, must be known. For Unitherm fire retardant paint, the following values can be used in determining the maximum steel temperature. Two-coat Unitherm application,  $d_i/\lambda_i = 0,075 \text{ m}^2\cdot^\circ\text{C h/kcal}$   $\{0,064 \text{ m}^2\cdot^\circ\text{C/W}\}$ . Three-coat Unitherm application,  $d_i/\lambda_i = 0,10 \text{ m}^2\cdot^\circ\text{C h/kcal}$   $\{0,086 \text{ m}^2\cdot^\circ\text{C/W}\}$ . These values have been determined using the results of standard fire tests. The values are clearly on the safe side and should be applicable also to other types of paint which are found in fire tests to exhibit at least the same fire resistance as Unitherm fire retardant paint.

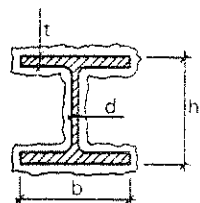
Table A7. Maximum steel temperature  $T_{s,max}$  ( $^{\circ}\text{C}$ ) for a steel structure insulated with mineral wool slabs, type Minwool 3060 or Rockwool 337 ( $\rho_i = 150 \text{ kg m}^{-3}$ ), as a function of effective fire load density  $q$  ( $\text{Mcal}\cdot\text{m}^{-2}$ ) [ $\text{MJ}\cdot\text{m}^{-2}$ ], effective opening area  $A\sqrt{h}/A_t$  ( $\text{m}^{1/2}$ ), structural parameter  $A_i/V_s$  ( $\text{m}^{-1}$ ), and insulation thickness  $d_i$  (mm)

q	$\frac{A\sqrt{h}}{A_t}$	$\frac{A_i}{V_s}$	$T_{s,max}$				q	$\frac{A\sqrt{h}}{A_t}$	$\frac{A_i}{V_s}$	$T_{s,max}$				q	$\frac{A\sqrt{h}}{A_t}$	$\frac{A_i}{V_s}$	$T_{s,max}$						
			$d_i$ 30	$d_i$ 50	$d_i$ 70	$d_i$ 30				$d_i$ 50	$d_i$ 70	$d_i$ 30	$d_i$ 50				$d_i$ 70						
20 {81}	0,01	200	325	250	200	40 {165}	0,02	100	370	275	215	60 {250}	0,02	50	400	255	220	90 {380}	0,04	50	415	295	220
		300	360	300	245			125	415	310	245			75	500	375	295			75	540	390	300
		400	415	335	275			150	455	345	270			100	565	440	350			100	620	465	365
		200	295	215	165			200	315	400	320			125	610	495	400			125	680	530	420
		300	355	265	210			300	385	475	390			150	640	530	440			150	725	580	465
		400	400	300	240			400	625	525	435			200	690	595	505			200	785	650	540
	0,04	200	300	205	150		0,04	100	300	205	155		0,04	75	355	250	190		0,06	75	370	260	195
		300	350	250	180			125	340	240	180			100	425	305	230			100	510	360	270
		400	400	320	260			150	380	270	205			125	485	350	270			125	570	410	315
		125	330	250	200			200	450	320	240			200	600	450	350			150	625	460	355
		150	355	270	225			300	535	400	300			300	690	550	430			200	710	530	420
		400	480	465	340			400	600	450	350			400	740	600	455			300	-	635	510
25 {105}	0,01	200	300	210	150	45 {180}	0,02	100	330	225	155	75 {315}	0,04	200	600	200	150	120 {500}	0,06	200	600	200	150
		300	350	260	205			125	415	325	215			100	360	250	185			100	450	310	230
		400	465	355	255			150	465	325	240			125	415	325	215			125	515	365	270
		200	300	210	150			200	350	265	200			200	540	385	285			150	570	400	300
		300	375	265	195			300	430	310	225			300	650	475	360			200	650	480	360
		400	430	310	225			400	500	340	230			400	710	540	415			300	765	585	450
	0,02	200	330	210	150		0,02	100	330	210	150		0,02	75	300	200	150		0,08	75	375	250	190
		300	390	250	170			125	370	250	180			100	360	250	185			100	450	310	230
		400	465	355	255			150	415	285	215			125	415	325	215			125	515	365	270
		200	300	210	150			200	500	340	250			200	540	385	285			150	570	400	300
		300	375	265	195			300	430	310	225			300	650	475	360			200	650	480	360
		400	430	310	225			400	500	340	230			400	710	540	415			300	765	585	450
30 {120}	0,01	75	310	230	175	50 {210}	0,02	100	330	225	155	75 {315}	0,04	200	600	200	150	120 {500}	0,06	200	600	200	150
		100	355	270	215			125	370	250	180			100	360	250	185			100	450	310	230
		125	390	305	245			150	415	285	215			125	415	325	215			125	515	365	270
		150	420	335	270			200	450	320	240			200	540	385	285			150	570	400	300
		200	460	375	315			300	495	340	250			300	605	435	305			200	650	480	360
		300	500	425	365			400	540	385	285			400	690	500	350			300	765	585	450
	0,02	75	310	230	175		0,02	100	330	210	150		0,02	75	300	200	150		0,08	75	375	250	190
		100	355	270	215			125	370	250	180			100	360	250	185			100	450	310	230
		125	390	305	245			150	415	285	215			125	415	325	215			125	515	365	270
		150	420	335	270			200	450	320	240			200	540	385	285			150	570	400	300
		200	460	375	315			300	495	340	250			300	605	435	305			200	650	480	360
		300	500	425	365			400	540	385	285			400	690	500	350			300	765	585	450
35 {147}	0,01	125	320	235	185	55 {210}	0,02	100	330	225	155	75 {315}	0,04	200	600	200	150	120 {500}	0,06	200	600	200	150
		150	355	260	205			125	370	250	180			100	360	250	185			100	450	310	230
		200	405	305	240			150	415	285	215			125	415	325	215			125	515	365	270
		300	480	370	300			200	450	320	240			200	540	385	285			150	570	400	300
		400	530	420	335			300	495	340	250			300	605	435	305			200	650	480	360
		400	520	460	405			400	540	385	285			400	690	500	350			300	765	585	450
	0,02	125	320	235	185		0,02	100	330	210	150		0,02	75	300	200	150		0,08	75	375	250	190
		150	355	260	205			125	370	250	180			100	360	250	185			100	450	310	230
		200	405	305	240			150	415	285	215			125	415	325	215			125	515	365	270
		300	480	370	300			200	450	320	240			200	540	385	285			150	570	400	300
		400	530	420	335			300	495	340	250			300	605	435	305			200	650	480	360
		400	520	460	405			400	540	385	285			400	690	500	350			300	765	585	450

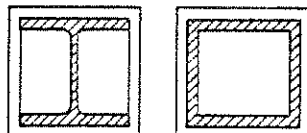


Table A8.  $A_i/V_s$  for different types of fire exposed, insulated steel structures

Column in a fire compartment

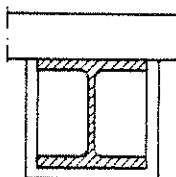


$$\frac{A_i}{V_s} = \frac{2h + 4b - 2d}{\text{steel cross section area}}$$



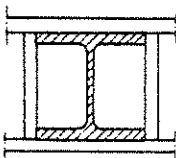
$$\frac{A_i}{V_s} = \frac{2h + 2b}{\text{steel cross section area}}$$

Column against a wall with a sufficient fire resistance



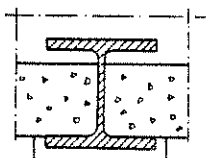
$$\frac{A_i}{V_s} = \frac{2h + b}{\text{steel cross section area}}$$

Column within a wall with a sufficient fire resistance



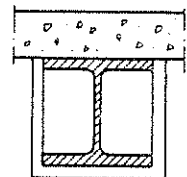
$$\frac{A_i}{V_s} = \frac{b}{bt} = \frac{1}{t}$$

Floor structure, composed of steel beams with a concrete slab, supported on the lower flange of the beams



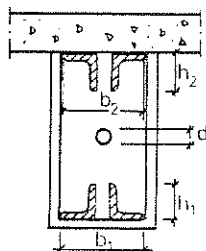
$$\frac{A_i}{V_s} = \frac{b}{bt} = \frac{1}{t}$$

Beams with a floor slab, supported on the upper flange of the beams



$$\frac{A_i}{V_s} = \frac{2h + b}{\text{steel cross section area}}$$

Floor slab beams of truss type ( $A_i/V_s$  is determined for each part of the truss)



$$\frac{A_i}{V_s} \text{ (lower flange)} = \frac{2b_1 + 2h_1}{\text{cross section area of lower flange}}$$

$$\frac{A_i}{V_s} \text{ (upper flange)} = \frac{b_2 + 2h_2}{\text{cross section area of upper flange}}$$

$$\frac{A_i}{V_s} \text{ (diagonal)} = \frac{h}{d}$$

Table A9. Maximum steel beam temperature  $T_{s,max}$  ( $^{\circ}\text{C}$ ) for a steel beam construction according to Fig. 20, with an insulation in the form of a suspended ceiling, as a function of effective fire load density  $q$  ( $\text{Mcal}\cdot\text{m}^{-2}$ ) [ $\text{MJ}\cdot\text{m}^{-2}$ ], effective opening factor  $A\sqrt{h}/A_t$  ( $\text{m}^{1/2}$ ), structural parameter  $F_s/V_s$  ( $\text{m}^{-1}$ ), and insulation parameter  $d_i/\lambda_i$  ( $\text{m}^2\cdot^{\circ}\text{C}\cdot\text{h}\cdot\text{kcal}^{-1}$ )<sup>c</sup>. The maximum temperature in the suspended ceiling is given in brackets [4]

q	$\frac{A\sqrt{h}}{A_t}$	$\frac{F_s}{V_s}$	Maximum steel temperature $T_{s,max}$ and ( ) maximum suspended ceiling temperature				q	$\frac{A\sqrt{h}}{A_t}$	$\frac{F_s}{V_s}$	Maximum steel temperature $T_{s,max}$ and ( ) maximum suspended ceiling temperature				
			$(d_i/\lambda_i)_{fact}$							$(d_i/\lambda_i)_{fact}$				
			0,05	0,10	0,20	0,30				0,05	0,10	0,20	0,30	
15 {63}	0,02	50	130	90	65	50	60 {250}	0,02	50	435	315	200	160	
		100	180	130	90	70			100	450	340	240	185	
		200	230	(470)	170	(440)			115	(410)	90	(390)	200	(500)
		300	260		190				130		100		200	
	0,04	50	100	70	45	40		0,04	50	340	225	145	110	
		100	150	(565)	100	(530)			65	(500)	50	(475)	140	(560)
		200	200		140				90		70		165	
		300	240		170				110		80		180	
	0,08	50	65	50	35	25		0,08	50	250	160	100	75	
		100	95	70	50	40			100	340	225	130	100	
		200	150	(675)	100	(630)			65	(590)	50	(570)	135	(625)
		300	190		125				90		60		155	
	0,12	50	40	35	30	25		0,12	50	190	120	75	60	
		100	60	45	40	(690)			40	(650)	30	(620)	80	(660)
		200	120	(735)	70				50		40		110	
		300	155		100				60		45		130	
25 {105}	0,02	50	200	140	95	75	90 {380}	0,04	50	475	330	205	150	
		100	260	185	125	100			100	510	370	250	190	
		200	300	(510)	225	(470)			155	(435)	120	(420)	210	(600)
		300	320		245				170		130		215	
	0,04	50	160	110	75	55		0,08	50	345	225	130	100	
		100	230	(600)	150	(565)			100	430	290	180	130	
		200	290		205	(530)			135	(500)	100	(475)	170	(650)
		300	325		235				155		115		190	
	0,08	50	115	75	50	40		0,12	50	550	400	260	200	
		100	160	(680)	110	(635)			70	(595)	55	(570)	220	(630)
		200	240		160				100	480	340	225	170	
		300	285		195				120		90		230	
	0,12	50	80	60	40	30		0,08	50	425	280	160	120	
		100	130	80	60	45			100	495	345	210	160	
		200	190	(740)	125	(690)			80	(650)	60	(620)	195	(670)
		300	235		160				100		75		205	
40 {168}	0,02	50	300	220	145	110	120 {500}	0,04	50	570	420	290	230	
		100	360	260	175	135			100	575	425	300	230	
		200	380	(560)	290	(520)			200	575	425	300	230	
		300	385		295				210		165		205	
	0,04	50	240	160	105	80		0,08	50	425	280	160	120	
		100	315	(645)	220	(600)			140	(560)	100	(535)	195	(670)
		200	375		270				180		135		205	
		300	390		290				195		150		205	
	0,08	50	170	110	70	55		0,12	50	425	280	160	120	
		100	245	(715)	160	(665)			100	495	345	210	160	
		200	335		220				140	(625)	75	(600)	195	(670)
		300	380		260				165		120		205	
	0,12	50	130	85	55	45		0,12	50	425	280	160	120	
		100	200	130	85	60			100	495	345	210	160	
		200	290	(750)	190	(700)			115	(660)	85	(630)	195	(670)
		300	340		225				145		100		205	

$C \begin{cases} 0,05 \text{ m}^3 \text{ } ^\circ\text{Ch/kcal} = 0,043 \text{ m}^3 \text{ } ^\circ\text{C/W} \\ 0,10 \text{ } & = 0,086 \text{ } & \\ 0,20 \text{ } & = 0,172 \text{ } & \\ 0,30 \text{ } & = 0,258 \text{ } & \end{cases}$

$$^c \begin{cases} 0,05 \text{ m}^2 \cdot ^{\circ}\text{C}\cdot\text{h}/\text{kcal} = 0,043 \text{ m}^2 \cdot ^{\circ}\text{C}/\text{W} \\ 0,10 \text{ } \gg \gg = 0,086 \text{ } \gg \gg \\ 0,20 \text{ } \gg \gg = 0,172 \text{ } \gg \gg \\ 0,30 \text{ } \gg \gg = 0,258 \text{ } \gg \gg \end{cases}$$

Table A10. Summary results of standard fire resistance tests on some types of suspended ceilings and connected values, derived from the test results, for  $(d_i/\lambda_i)_{\text{eff}}$  and critical temperature of the ceilings [4]

No	Make	Material	Resistance time in standard fire test (min)	Remarks	Estimated $(d_i/\lambda_i)_{\text{eff}}$ $\left(\frac{\text{m}^2}{\text{kcal}}\right)$	Estimated critical suspended ceiling temperature (°C)
1	Gyproc	2x13 mm gypsum plaster slabs no glass fibre reinforcement	30-40	All tests were discontinued because the suspended ceiling fell down. The critical temperature had not been reached in the steel girders	0,075	625
2		1x13 mm gypsum plaster slabs 0,25% g f r	48		0,075	650
3		1x16 mm gypsum plaster slabs 0,25% g f r	48		0,10	650
4		2x13 mm gypsum plaster slabs 0,25% g f r	60		0,13	650
5		3x13 mm gypsum plaster slabs 0,25% g f r	75-80		0,25	625
6		2x20 mm gypsum plaster slabs 0,25% g f r	80	All tests were discontinued for the same reason as above. The gypsum plaster slabs were not reinforced	0,30	625
7	WST	2x13 mm gypsum plaster slabs with 13 mm mineral wool between them	45		0,30	550
8		2x13 mm gypsum plaster slabs with 13 mm mineral wool between them	50		0,30	550
9		2x13 mm gypsum plaster slabs with 43 mm straw between them	47		0,30	550
10		2x13 mm gypsum plaster slabs with 43 mm straw between them	54		0,30	550
11	Ingenjör-firma Zero	Soundex special suspended ceiling tiles. Cast glass fibre reinforced gypsum plaster tiles with "ridges" in a grid pattern. Tile thickness 18 mm, at the ridges 38 mm	90	Parts of the ceiling fell down after 90 minutes. Max. steel temperature approx. 440°C	0,15	700
12	Consensus	Armstrong 13 mm thick	30	No visible damage to suspended ceiling. Max steel temperature about 450 °C	0,05	550
13		Mineral wool acoustic 16 mm thick	80		0,075	650 <sup>a</sup>
14		Type minaboard 13 mm thick	85		0,075	650 <sup>a</sup>
15	Dansk Eternitfabrik	Deflamit-Asbestolux (9 mm Deflamit + 15 mm mineral wool + 8 mm eternit)	50	No visible damage to suspended ceiling. Max steel temperature about 300 °C	0,20	675 <sup>a</sup>
16	Nordakustik	Celotex Acoustiformat 15 mm thick glass fibre slab	90		0,10	650 <sup>a</sup>
17	Rockwool	Rockfon Decor 85l (15 mm thick mineral wool slab)	60	No visible damage to suspended ceiling. Max steel temperature about 450 °C. The test was discontinued because the suspended ceiling fell down. The critical temperature had not been reached in the steel girders.	0,20	600

<sup>a</sup> No damage to the suspended ceiling. Calculated temperature in the suspended ceiling when the test was discontinued.

Table A11. Load values to be applied in a differentiated, analytical, structural fire engineering design [2], [4], [6].

It is to be proved that the load-bearing structure or structural member does not collapse during the complete process of fire development for the most unfavourable combination of dead load, live load, snow load and wind load. On the assumption that the design fire load density is chosen according to Table A1, the following load values are to be applied. The values include a safety factor which roughly takes into account the probability of a fully developed fire and the probability of the presence of the maximum load at the fire occasion.

(a) Complete evacuation of occupants not certainly anticipated

Following values shall be applied for the live load.

Type of fire compartment	Permanent loading $\text{kN.m}^{-2}$	Movable loading $\text{kN.m}^{-2}$
Dwellings, hotels and hospitals	0.5	1.0
Offices	0.5	1.5
Schools (lecturing rooms)	0.5	1.5
Schools (corridors)	0.5	2.5
Assembly-rooms	1.0	2.0
Libraries	1.0	2.0

For the snow load, permanent and movable loading values shall be in accordance to the general loading regulations.

For the wind load, values shall be applied which correspond to a velocity pressure = 50% of the velocity pressure specified in the general loading regulations.

(b) Complete evacuation of occupants certainly anticipated

Following values shall be applied for the live load. Snow and wind load according to (a).

Type of fire compartment	Permanent loading $\text{kN.m}^{-2}$	Movable loading $\text{kN.m}^{-2}$
Dwellings, hotels and hospitals	0.5	0.5
Offices	0.5	0.8
Schools (lecturing rooms)	0.5	0.8
Schools (corridors)	0.5	0.8
Assembly-rooms	1.0	0.8
Libraries	1.0	2.0

Due consideration shall be taken to the local increase of the live load in connection with an evacuation of the building or a removal of people to a safe place of refuge within the building.